THESIS APPROVAL

GRADUATE SCHOOL, KASETSART UNIVERSITY

Doctor of Philosophy (Agricultural Biotechnology)

DEGREE

Agricultural Biotechnology — **FIELD**

Interdisciplinary Graduate Program — **PROGRAM**

TITLE: Effects of Antibiotic Coated High Porous Calcium Sulfate Beads on Osteomyelitis Management: *in vitro* and *in vivo* Studies

NAME: Mr. Chaiyakorn Thitiyanaporn

THIS THESIS HAS BEEN ACCEPTED BY

_____ **THESIS ADVISOR**

(Associate Professor Naris Thengchaisri, Ph.D.)

_____ **COMMITTEE MEMBER**

(Assistant Professor Pareeya Udomkusonsri, Ph.D.)

_____ **GRADUATE COMMITTEE CHAIRMAN**

(Assistant Professor Sermsiri Chanprem, Ph.D.)

APPROVED BY THE GRADUATE SCHOOL ON _____

DEAN

(Associate Professor Gunjana Theeragool, D.Agr.)

THESIS

EFFECTS OF ANTIBIOTIC COATED HIGH POROUS CALCIUM SULFATE BEADS ON OSTEOMYELITIS MANAGEMENT: *in vitro* AND *in vivo* STUDIES

CHAIYAKORN THITIYANAPORN

A Thesis Submitted in Partial Fulfillment of
The Requirement for the Degree of
Doctor of Philosophy (Agricultural Biotechnology)
Graduate School, Kasetsart University
2013

Chaiyakorn Thitiyanaporn 2013: Effects of Antibiotic Coated High Porous Calcium Sulfate Beads on Osteomyelitis Management: *in vitro* and *in vivo* Studies. Doctor of Philosophy (Agricultural Biotechnology), Major Field: Agricultural Biotechnology, Interdisciplinary Graduate Program. Thesis Advisor: Associate Professor Naris Thengchaisri, Ph.D. 94 pages.

The high porous calcium sulfate (HPCS) bead was created in this study by salt leaching technique. In the first study, variations of the ratio between calcium sulfate (CS) and sodium chloride salt made the different porosity levels of CS bead with determine the ceftazidime elution pattern from the CS beads. The maximum ratio of CS per sodium chloride was 1:1 w/w that could increase the total porosity level up to 50%. The highest porosity level of CS is the high porous calcium sulfate (HPCS) bead. The HPCS bead could provide total amount of the ceftazidime as same as the native calcium sulfate (NCS) bead with a shorter period than NCS bead. In the second study, the gentamicin impregnated polymethylmethacrylate (GI-PMMA) bead with gentamicin coated PMMA (G-PMMA) were compared with gentamicin coated NCS (G-NCS) and gentamicin coated HPCS (G-HPCS) beads on gentamicin releasing. G-NCS and G-HPCS beads could provide the gentamicin concentration higher than GI-PMMA and G-PMMA beads and also found that the coating technique could be used only in CS bead in this study. For the third study, the efficiency of GI-PMMA, G-NCS and G-HPCS beads were compared in the management of osteomyelitis in a rat model. The results showed that G-HPCS bead could be used for the osteomyelitis management as G-NCS bead whereas G-PMMA bead had to be removed from the bone and created a defect on the bone cortex.

The results of studies showed that the HPCS bead is a new type of CS bead that can be used as an antibiotic carrier for osteomyelitis management. In addition, the HPCS bead also has a positive effect for the new bone regeneration.

_____ _____ ____ / ____ / ____

Student's signature Thesis Advisor's signature

ACKNOWLEDGEMENTS

I would like to express my sincere gratefulness and deep appreciation to Associate Professor Dr. Naris Thengchaisri, my thesis advisor and Assistant Professor Dr. Pareeya Udomkusonsri, my thesis co-advisor for their warm support, kindness, excellent advice, valuable guidance, encouragement and suggestion.

I would like to sincerely thank my colleagues of the Department of Companion Animal Clinical Sciences, Faculty of Veterinary Medicine, Kasetsart University and the Veterinary Teaching Hospital, Faculty of Veterinary Medicine, Kasetsart University, Bangkhen Campus for providing facilities and all instruments during my study. I gratefully thank my wife Dr. Tassanee Jaroensong for her encouragement during my study.

This thesis was supported by the Center for Agricultural Biotechnology, Kasetsart University, Center of Excellence on Agricultural Biotechnology, Science and Technology Postgraduate Education and Research Development Office, Commission on Higher Education, Ministry of Education. (AG-BIO/PERDO-CHE) and the Strategic Scholarships Fellowships Frontier Research Network, Office of the Higher Education Commission, Ministry of Education.

Finally, I am especially appreciated my parents, my sisters and brother for their love, entirely care, continuing encouragements. The usefulness of this thesis, I dedicate to my parents, all of my teachers and animals.

Chaiayakorn Thitiyanaporn

February 2013

TABLE OF CONTENTS

Page

LIST OF TABLES

LIST OF FIGURES

LIST OF FIGURES (Continued)

LIST OF FIGURES (Continued)

LIST OF FIGURES (Continued)

LIST OF ABBREVIATIONS

AD	=	architecture deformation
AIDS	=	acquire immune deficiency syndrome
ANOVA	=	analysis of variance
ATCC	=	American type culture collection
BMP-2	=	bone morphogenetic protein-2
BMP-7	=	bone morphogenetic protein-7
BMPs	=	bone morphogenetic proteins
°C	=	degree Celsius
$CaSO_4.1/2H_2O$	=	calcium sulfate hemihydrate
$CaSO_4.2H_2O$	=	calcium sulfate dihydrate
CFU	=	colony forming unit
cm	=	centimeter
CO_2	=	carbon dioxide
CRP	=	C-reactive protein
CS	=	calcium sulfate
CT	=	computed tomography
DMEM	=	Dulbecco's Modified Eagle Medium
DNA	=	deoxyribonucleic acid
EDTA	=	ethylenediaminetetraacetic acid
ESR	=	erythrocyte sedimentation rate
FDG	=	fluorine-18-fluoro-2-deoxy-D-glucose
G-HPCS	=	gentamicin coated high porous calcium sulfate
G-NCS	=	native calcium sulfate
G-PMMA	=	gentamicin coated polymethylmethacrylate
GI-PMMA	=	gentamicin impregnated polymethylmethacrylate
H&E	=	hematoxylin and eosin
HIV	=	human immunodeficiency virus
HPCS	=	high porous calcium sulfate

LIST OF ABBREVIATIONS (Continued)

H_2O	=	water
h-OBs	=	human osteoblast
IGFs	=	insulin-like growth factors
K-wire	=	kirchner wire
kg	=	kilo gram
kV	=	kilo voltage
MC3T3-E1	=	mouse osteoblast
mg	=	milligram
MIC	=	mimimum inhibitory concentration
min	=	minute
ml	=	milliliter
mm	=	millimeter
MPa	=	megapascal
MRI	=	magnetic resonance imaging
MRSA	=	methicilliin resistance *Staphylococcus aureus.*
N	=	newton
NCS	=	native calcium sulfate
NMF	=	new bone formation
PBS	=	phosphate buffer saline
PCR	=	polymerase chain reaction
PDGF	=	platelet derived growth factor
PE	=	periosteal reaction
PET	=	positron emission tomography
PMMA	=	polymethylmethacrylate
PRA	=	percentage of radiolucent area
R	=	correlation coefficient
rh-BMP	=	recombinant human bone morphogenetic protein
RNA	=	ribonucleic acid
RS	=	radiological score

LIST OF ABBREVIATIONS (Continued)

SD	=	standard deviation
SEM	=	scanning electron microscope
STD	=	soft tissue deformation
TGFs	=	transforming growth factors
TGF-β	=	transforming growth factor-β
w/v	=	weight per volume
w/w	=	weight per weight
WBS	=	widening of the bone shaft
µg	=	microgram
µl	=	microliter
µm	=	micrometer

EFFECTS OF ANTIBIOTIC COATED HIGH POROUS CALCIUM SULFATE BEADS ON OSTEOMYELITIS MANAGEMENT: *IN VITRO* AND *IN VIVO* STUIDES

INTRODUCTION

Osteomyelitis is an inflammatory process accompanied by bone destruction and caused by microorganism infection (Lew *et al*., 2004). The infection can be limited to a single portion of the bone or can involve several regions, such as periosteum, marrow, cortex and the surrounding tissues. The treatments of osteomyelitis classically involve surgical debridement of necrotic tissue, irrigation, obliteration of dead space, bone repair, adequate soft tissue coverage and systemic antimicrobial administration for 4-6 weeks (Lazzarini *et al*., 2004; Mader *et al*., 1999). Although these methods can eradicate or suppress the infection process, the disadvantages of intravenous antibiotic administration are including a failure of catheter, infection, systemic toxicity and high cost. Furthermore, the necrosis of the infected bones tissue is results from decreasing of vascularity causes compromising the effectiveness of systemic antibiotic therapy (Mader *et al*., 2002). Antibiotic impregnated polymethylmethacrylate (PMMA) beads are clinically used in various area including joint replacement surgery and commonly used for standard treatment of local infected tissue, especially osteomyelitis (Gondusky *et al*., 2009; Kelsey *et al*., 1995; Koo *et al*., 2001; Malizos *et al*., 2010; Roeder *et al*., 2000). However, disadvantages of PMMA used in osteomyelitis management were the requirement for surgical removal (Mader *et al*., 2002; Nelson *et al*., 2002), enhancement of bacterial colonization (Mader *et al*., 2002), higher cost of management and release of toxic substance during setting (Santschi *et al*., 2003). Unlike PMMA, the calcium sulfate beads have been used in the *in vitro* and *in vivo* studies as a vehicle to deliver the antibiotics, growth factors and other pharmacologic agents (Ham *et al*., 2008; Kanellakopoulou *et al*., 2009; Santschi *et al*., 2003; Thomas *et al*., 2009; Xie *et al*., 2009). Also antibiotic impregnated calcium sulfate beads have been used in medical practices, especially for the treatment of osteomyelitis (Ham *et al*., 2008; Kanellakopoulou *et al*., 2009). A local

antibiotic delivery system has been employed because it provides higher local antibiotic concentration than parenteral antibiotic administration; furthermore, an application of local antibiotics also reduces the risk of systemic side effects and aids dead space management (Gitelis *et al*., 2002).

In osteomyelitis lesion, the necrotic tissues were occurred from vascular damage. Calcium sulfate is a biomaterial that can provide a calcium ion during new bone regeneration and a scaffold for the osteogenic cell attachment. The implanted calcium sulfate bead can be totally resorbed with minimal inflammation (Thomas and Puleo, 2009). In addition, the beneficial effects of calcium sulfate on osteoconductive activity leads for using this material in both orthopedic and dental procedures (Bahn *et al*., 1966; Damien *et al*., 1991; Peltier *et al*., 1961). Calcium sulfate can be applied as a binder for bone grafting; it facilitated bone healing and prevented the loss of the grafting material in a rabbit model (Orsini *et al*., 2004). The osteoconductive mechanisms of calcium sulfate are involved in a direct source of calcium to the bone defect (Ruhaimi *et al*., 2001) and in a rapid rate of resorption which allows an earlier ingress of osteoprogenitor cells (MacNeill *et al*., 1999).

High porosity and interconnectivity pores are the major requirements for bone substitute materials; m*aterials* with *proper porosities* and pore sizes could facilitate cell attachment, cell ingrowth and promote a uniform cell distribution with the adequate transportation of nutrients and cellular waste products (Hou *et al*., 2003). Micropores allow a migration of endothelial cells, promote a differentiation of osteoblasts and osteoprogenitor cells, promote vascularisation, and contribute to an osteoblast proliferation and differentiation (Kusmanto *et al*., 2008). The pore size of the material is also a significant factor for bone regeneration. The minimum pore size diameter required for bone regeneration is approximately 100 μm (Hulbert *et al*., 1970). The porosity of the material can be calibrated with various techniques such as a leaching of soluble particle (Hou *et al*., 2003; Reignier and Huneault., 2006; McLaren *et al*., 2007), the mechanical and the chemical techniques (Frame *et al*., 1975; Shiramizu *et al*., 2008). Leaching of salt technique is an effective technique to control the amounts and sizes of pores, which

determined by the amount and size of the particle (Hou *et al*., 2003). Porosity of the material is not only important to osteogenesis but also positively influences the dissolution permeability of drugs which affects the antibiotic elution from biomaterials (McLaren *et al*., 2004; Schurman *et al*., 1978).

Various antibiotics were used to cooperate with antibiotic beads including aminoglycosides, β-lactam agents, and quinolones (Doadrio *et al*., 2004; Ham *et al*., 2008; Kanellakopoulou *et al*., 2009; Nandi *et al*., 2009; Santschi and McGarvey 2003; Tuzuner *et al*., 2007). Ceftazidime, a β-lactamase-stable third generation of cephalosporin in solution form, was employed for making antibiotic beads because it is a broad spectrum antibiotic and can inhibit most of the pathogens that cause osteomyelitis, especially when caused by *Pseudomanas* infection (Bach *et al*., 1987; Eron *et al*., 1983). In addition, gentamicin is frequently used in an antibiotic releasing bead, since gentamicin has a broad spectrum antimicrobial activity, highly solubility and resistance to a high temperatures required to create the PMMA and calcium sulfate dihydrate settings (Wahlig *et al*., 1980).

The hypothesis of this study were the salt leaching technique could increase porosity level of calcium sulfate bead, the releasing of antibiotic had been alternated in high porous calcium sulfate bead, the high porous calcium sulfate was compatibility with human osteoblast and the high porous calcium sulfate bead could be used as antibiotic carrier for managing osteomyelitis. Various porosity levels of calcium sulfate bead were studied in ceftazidime releasing in *in vitro* study. The high porous calcium sulfate (HPCS) bead show the highest efficiency on ceftazidime release. The gentamicin coated HPCS bead was continuing *in vitro* studied compare with gentamicin impregnated PMMA bead, gentamicin coated PMMA bead and gentamicin coated native calcium sulfate bead. After that, the HPCS was studied in rat osteomyelitis model for comparison the capability of osteomyelitis management with commercial gentamicin impregnated PMMA bead and gentamicin coated native calcium sulfate bead.

OBJECTIVES

1. To develop a new type of calcium sulfate bead for as local antibiotic carrier**.**

2. To compare the efficiency of high porous calcium sulfate bead with commercial antibiotic impregnated PMMA bead, antibiotic coated commercial PMMA bead and antibiotic coated native calcium sulfate bead on antibiotic releasing in *in vitro* study**.**

3. To compare the capability of high porous calcium sulfate bead with commercial antibiotic impregnated PMMA bead and antibiotic coated native calcium sulfate bead in rat osteomyelitis model**.**

LITERATURE REVIEW

1. Osteomyelitis

1.1 Definition

Osteomyelitis is an inflammatory disease of bone and marrow cavity (Mast *et al*., 2002). It is heterogenous in pathophysiology, clinical presentation, and management (Sia *et al*., 2006). Usually, it is limited to a single bone, however, it rarely can be multifocal lesions (McNally *et al*., 2010).

1.2 Etiology

Staphylococcus aureus can cause all types of osteomyelitis and it is the causal organism in over one-third of acute cases and half of all vertebral infections (McNally *et al*., 2010). *S. aureus* is the commonest organism in acute osteomyelitis, followed by *Enterococci, Enterobacteriacae, Streptococci*, and anaerobic bacteria (Gotz *et al*., 2002). The early stages of infection are characterized with a race between the bacteria and the host defenses to control the local environment. If the inoculum size is large enough or the host defenses are impaired, the infection in the tissue can occur. Moreover, the presence of multiple organisms may cause of osteomyelitis. The production of streptolysin by relatively low-virulence Streptococcus species may cause potentially life-threatening soft tissue infections in the presence of the other organisms. The biofilm is an anionic, extracapsular, polysaccharide slime produced by bacteria, to protect them from antibiotic therapy and host clearance mechanisms. Expression of biofilm has been characterized in Staphylococcus species, *Pseudomonas aeruginosa*, and *Streptococcus mutans* (Gotz *et al*., 2002). In addition, collagen binding collagen produced by *S. aureus* have a contributory role in hematogenous infection (Elasri *et al*., 2002). Host physiology is the body's ability to control the local and systemic insults in the wound healing. In HIV and AIDS, osteomyelitis is the third most common infective presentation. The relationship

between bony stability and susceptibility to infection has been shown in an animal model. When fixation was applied to fractures in rabbits using a dynamic compression plate (stable group) or a loose-fitting intramedullary rod (unstable group) then inoculated with a standard inoculum of *S. aureus*, the stable fixation group demonstrated a lower incidence of subsequent infection (Cierny *et al*., 2003).

1.3 Classification

Because of the wide variability in the etiology of osteomyelitis, the classification of osteomyelitis based on duration of the disease (acute or chronic) and pathogenesis of the disease: 1) hematogenous osteomyelitis, 2) osteomyelitis secondary to a contiguous focus of infection and 3) osteomyelitis associated with peripheral vascular disease (Waldvogel *et al*., 1970). In 1984, the classification system attempted to divide osteomyelitis based upon anatomy and structural factors into 4 groups: hematogenous osteomyelitis, osteomyelitis with united fracture, osteomyelitis with nonunion and osteomyelitis without fracture (Kelly *et al*., 1984). Subsequent classification systems introduced to divide osteomyelitis based upon the structural and anatomic status of the tibia after adequate soft tissue and skeletal debridement and the resultant impact upon treatment options and rehabilitation time (May *et al*., 1989). Type I tibial osteomyelitis occurs where functional loading of the tibia and fibula can still occur. The rehabilitation time was estimated at 6-12 weeks. Type II tibial osteomyelitis occurs when there is an intact tibia after debridement but bone grafting is required for structural support. The rehabilitation time was estimated at 3-6 months. Type III osteomyelitis has a tibial defect less than or equal to 6 cm long with an intact fibula. The rehabilitation time was estimated at 6-12 months. Type IV osteomyelitis has a tibial defect greater than 6 cm long with an intact fibula. The rehabilitation time was estimated at 12-18 months. Type V osteomyelitis has a tibial defect greater than 6 cm long without an intact useable fibula. The rehabilitation time was estimated greater than18 months. Recently, Cierny and Mader's classification system based upon the degree of anatomic involvement and host physiology is the most widely used in orthopedic literature (Cierny *et al*., 2003). Stage 1, or medullary, is infected intramedullary surfaces of bone or acute hemoatogenous

osteomyelitis. Stage 2, or superficial, is defined similar to contiguous focus osteomyelitis when an exposed infected necrotic surface of bone lies at the base of a soft tissue wound. Stage 3, or localized, is characterized by full thickness cortical sequestration requiring surgical removal without compromising bony stability. Stage 4, or diffuse, is a through and through infection requiring intercalary resection of bone and loss of stability. The physiologic class of the host is based upon the presence of factors that further support infection, such as malnutrition, diabetes mellitus, tobacco use, venous stasis, arteritis, and radiation fibrosis. The host is classified into 3 groups: A, B, and C hosts. “A” hosts have normal physiologic responses to infection. “B” hosts have either systemically and/or locally active impairment of normal physiological responses. “C” hosts have the disease itself when the results of treatment are more compromising to the patient than the disability. Staging of osteomyelitis in this manner allowed for a treatment strategy which defined optimal treatment modalities and prognosis for each stage.

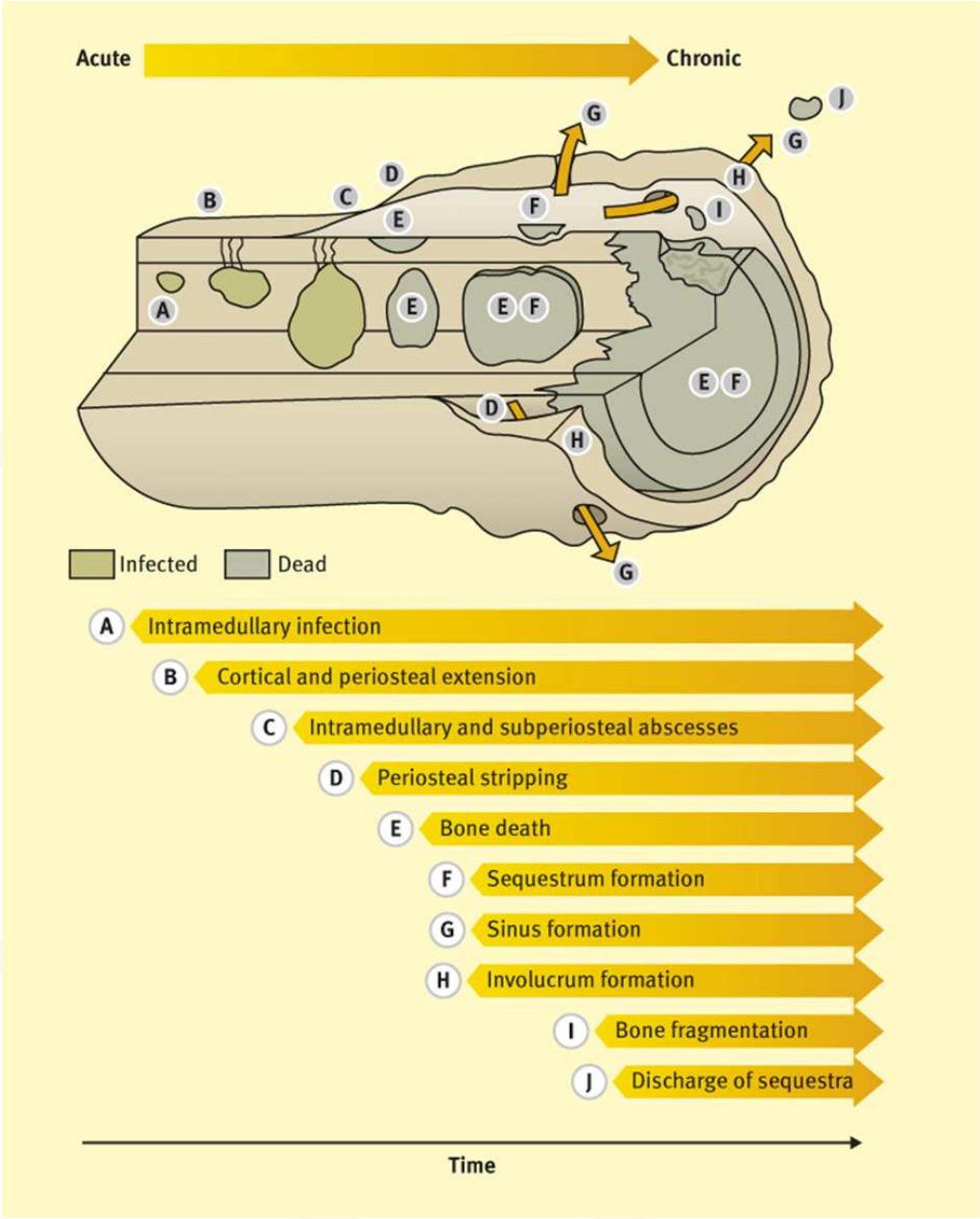

Figure 1 Schematic diagram of the evolution of bone infection from acute medullary disease to chronic osteomyelitis with dead bone, involucrum, sinuses and discharge.

Source: McNally and Nagarajah (2010)

1.4 Diagnosis

A detailed history and physical examination are essential for the approach to the patients with suspected osteomyelitis. A particular attention on physical examination should be paid to the signs of acute inflammation, such as pain, swelling, increased limb temperature, erythema, and loss of function. There are no specific blood tests to confirm the diagnosis of bone infection. In acute osteomyelitis, the white blood cell count, C-reactive protein (CRP) and erythrocyte sedimentation rate (ESR) level are usually elevated but are often normal in chronic osteomyelitis (McNally and Nagarajah, 2010). The concentration of CRP, synthesized by the liver in response to any infection, appears more reliable for follow up the response to treatment. The concentration increases within hours of infection and return to normal within a week after adequate treatment has begun in most cases (Unkila-Kallio *et al*., 1994). However, both CRP concentration and erythrocyte sedimentation rate may be higher than normal for reasons other than osteomyelitis. Concentrations of calcium, phosphate and alkaline phosphatase are normal in osteomyelitis in contrast to metastatic or some metabolic bone diseases (Lew *et al*., 2004).

The gold standard diagnostic tests are histological assessment and microbiological culture of the infecting organism from more than one deep specimen, taken with strict aseptic precautions in a patient who has not received any antimicrobial agents for at least 10 days. Superficial sinus tract culture has been shown to be misleading and has a poor correlation with deep tissue flora because the isolates may include non-pathogenic microorganisms that are colonizing the site. Whenever bone biopsies are done, the samples should be processed for aerobic and anaerobic cultures (Lew and Waldvogel, 2004). Therefore, the choice of antibiotic should not be depended on superficial cultures (Mast and Horwitz, 2002; McNally and Nagarajah, 2010). Recently, molecular techniques become a diagnostic method for osteomyelitis. In 2007, a research of Fihman, V. et al. show that the PCR technique can be used for diagnosis the cause of osteomyelitis including *Staphylococcus aureus, Streptococcus pyogenes, Streptococcus algalactiae, enterococcus faecalis, Salmonella enteric, Escherichia coli,*

Pseudomonas aeruginosa, and fastidious bacteria like *Neisseria gonorrhoeae* and *Fusobacterium nucleatum* (Fihman *et al*., 2007). Some laboratories are now advocating the use of specific genetic probes for identification of bacterial DNA and RNA. This will be the method of diagnosis in the future but is not universally accepted at present. In chronic osteomyelitis, histology can confirm the diagnosis in cases with negative culture by the demonstration of acute and chronic inflammatory cells, dead bone, active bone resorption and remodeling, and the present of small sequestra (McNally and Nagarajah, 2010). The presence of neutrophils in significant amount is indicative of infection. More than 5 neutrophil per high power field indicates infection, with sensitive of 43-84% and specificity of 93-97% (Abdul-Karim *et al*., 1998).

Conventional radiography is necessary diagnostic tools at both presentation and follow-up. Plain films show soft tissue swelling, narrowing or widening of joint spaces, bone destruction and periosteal reaction. However, bone destruction is not appearing on plain films until after 10-21 days of infection (Kaim *et al*., 2000; Santiago *et al*., 2003). In addition, ultrasonography can be useful for early diagnosis in acute osteomyelitis or for detection of a purulent collection in soft tissue (Howard *et al*., 1995; Kaiser *et al*., 1994; Mah *et al*., 1994). Computed tomography (CT) and magnetic resonance imaging (MRI) are a sensitive investigation for bone destruction of medullar, periosteal reaction, cortical destruction, articular damage, and soft tissue involvement, even when conventional radiographs are normal. Fine cut CT can aid in the design of surgical approaches to excise disease but it has little place in initial diagnosis of infection. MRI, however, is more useful than CT for soft tissue assessment. MRI is the single most effective investigation in the early inflammatory change and infection. It is limited by the presence of metal implants and requires considerable skill in interpretation in chronic osteomyelitis. However, it can over estimate the extent of medullary infection in the acute phase due to widespread bone edema of obscuring the margins of the active infection. Additionally, post operative MRI changes may persist for months or years and can be difficult to distinguish from recurrent infection. Currently, various radiopharmaceuticals are used for bone scintigraphy methylene diphosphonate binds to sites of increased bone metabolic activity and is highly sensitive in the early detection of

acute osteomyelitis. Leukocyte scanning with radiolabelled blood cells (leukocytes or granulocytes labeled with indium-111 or technetium-99m) or specific antibodies has been used for imaging of infection with reported high sensitivity and specificity (Mudun *et al*., 1995; Peters *et al*., 1998). The limitation of this imaging procedure should be mentioned because diabetic arthropathy, gout, trauma and surgery can give the false positive results. In additional imaging procedure, positron emission tomography (PET) with fluorine-18-fluoro-2-deoxy-D-glucose (FDG) combined with CT scan appears particularly promising for delineation of lesions and the concomitance inflammatory and infectious activity (Robiller *et al*., 2000; Schmitz *et al*., 2000).

1.5 Treatment

Optimal treatment and outcome of osteomyelitis depend upon the relationship between 3 factors, which are known as Klemm's Triad: 1) the virulence and the antibiotic sensitivity of the organism; 2) the viability and stability of the bone; and 3) the condition of the soft tissue envelope (Brady *et al*., 2006). The treatment of osteomyelitis in most patients requires optimal parenteral antibiotic therapy, surgical removal of all necrotic tissue and bone culture for determination the antibiotic according to the drug sensitivity test. Generally, the antibiotic therapy should be continued for at least 6 weeks (Gentry *et al*., 1997). For acute osteomyelitis, the early diagnosis is an importance. Blood culture and high dose of intravenous antibiotic given should be active against *S. aureus*, *Streptococci* and Gram-negative rods such as *E.coli*. Cephalosporin, clindamycin or a combination of flucloxacillin and gentamicin may be used. Vancomycin should be substituted if there is the possibility of methicillin resistance *Staphylococcus aureus* (MRSA) infection. The intravenous antibiotic can be converted to oral therapy after 72 hours (McNally and Nagarajah, 2010).

Chronic bone infection is hard for management. Since, the antibiotic alone cannot eradicate the bacteria from the infected site. Since, extensive bone infection involves in many part of bone and dead tissues are developed. In some case, the pathologic fracture may happen from bone structure destruction. Surgical treatment is

important for debridement and excision of infected tissue, bone sampling, bone stabilization, dead space management and soft tissue covering (McNally and Nagarajah, 2010). The dead space can be filled with an antibiotic-loaded carrier to deliver the high concentration of antimicrobial directly to the site of the infection. Most will elute the drug at therapeutic levels for several weeks. Absorbable and non-absorbable carriers are available. Originally, Klemm described the use of PMMA beads as a carrier for gentamicin. These are provided on wire strings and can be molded to fit into many spaces. They can be placed with the end of the string protruding from the wound and gradually removal or can be buried in the bone, permanently, or for later removal during secondary reconstruction (Klemm *et al*., 1993). PMMA can also be formed into antibiotic-loaded rods to fill the whole medullary cavity of the long bones or it can be implanted as a temporary block spacer across joint or the diaphysis pending staged bone defect management. PMMA is available ready mixed with gentamicin or vancomycin. Other antibiotics can be added but must be heat stable up to at least 70 °C. However, many disadvantages are revealing in PMMA such as it has to be removed after a period of time, support bacterial growth, decrease bone mass and trigger inflammatory response (Meyer *et al*., 1998). In addition, implantation of a medical vehicle may compromise local immune system directs its activity against the foreign implant instead of invading pathogen (Kaya *et al*., 2011). For the absorbable carrier, the collagen carriers with gentamicin and calcium sulfate pellet with tobramycin are produced commercially. Calcium sulfate can be hand mixed and combined with almost any antibiotics as it does not heat up to any extent during curing. It can be used in a wide variety of bone spaces and dissolves at a predictable rate giving very high antibiotic levels for up to 8 weeks. Additionally, there is some evidence that it is osteoconductive, allowing bone ingrowth into the resection defect (McNally and Nagarajah, 2010).

2. Calcium sulfate

2.1 General information

Calcium sulfate is an inexpensive and abundant material. Calcium sulfate or gypsum is a mineral consisting of calcium sulfate dihydrate ($CaSO_4.2H_2O$). The gypsum is heated to 110 °C. it losses water in the process known as calcination. The result of this process is calcium sulfate hemihydrates ($CaSO_4.1/2H_2O$) and it is also known as plaster of Paris (1).

$$CaSO_4.2H_2O \longrightarrow CaSO_4.1/2H2O + 1\ 1/2\ H_2O \quad (1)$$

The calcium sulfate hemihydrates exist in two forms, α andβ, which differs in crystal size, surface area and lattice imperfections. The physical properties of α-hemihydrate form are the dental stone from which diagnostic casts are constructed. It is hard and relative insoluble when compare with the β-hemihydrate. The β-hemihydrate is characterized by an aggregate of irregular crystals with interstitial capillary pores (Figure 2), whereas the α-hemihydrate contains cleavage fragments, rod and prism-shaped crystals (Figure 3) (Thomas and Puleo, 2009).

When calcium sulfate hemihydrate is mixed with water, the calcium sulfate is formed with exothermic reaction (2). The calcium sulfate hemihydrate is dissolved; a two phase suspension of hemihydrates particles in saturated aqueous solution is formed. The solution becomes supersaturated with dihydrate crystal nucleate in the suspension and forms a precipitate. Nucleation and crystal growth continue until the solution is no longer saturate, leading to further dissolution of the hemihydrates. Alternatively, dissolution and precipitation continue, with growth of existing crystals or nucleation of the new crystal (Thomas and Puleo, 2009).

$$CaSO_4.1/2H_2O + 1\ 1/2\ H_2O \longrightarrow CaSO_4.2H_2O + \text{heat} \quad (2)$$

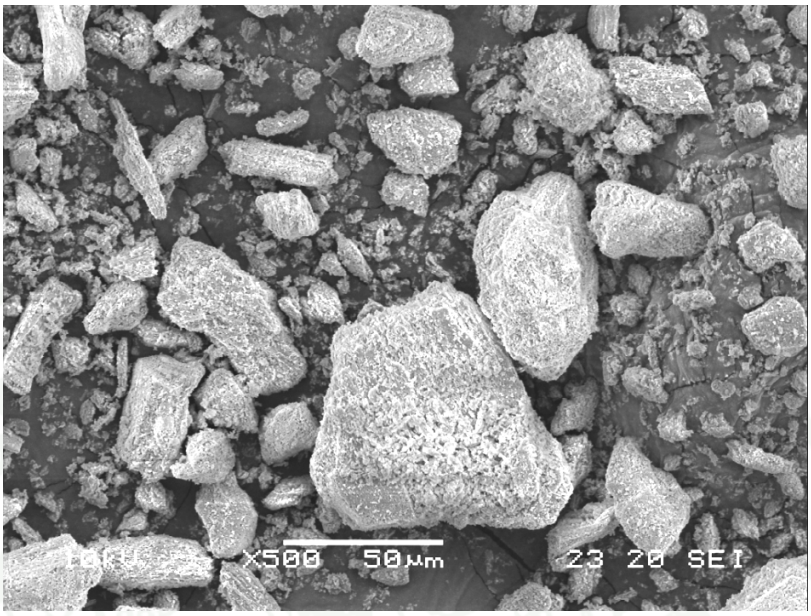

Figure 2 Powder particles of plaster of Paris (β-hemihydrate). Crystals are spongy and irregular in shape (×500).

Figure 3 Powder particles of dental stone (α-hemihydrate). Crystals are prismatic and more regular in shape than those of plaster. (×400).

Source: Anusavice (2003)

However, the calcium sulfate can be transformed into various types depending on the temperature. When the calcium sulfate dihydrate (Gypsum) is heat at 110-130 °C, it will be transformed to plaster of Paris. The plaster of Paris can be transformed to hexagonal anhydrite and orthorhombic anhydrite, respectively when the temperature is increasing as below equation (3).

$$\underset{\text{Gypsum}}{CaSO_4.2H_2O} \xrightarrow{1} \underset{\text{Plaster or stone}}{CaSO_4.1/2H_2O} \xrightarrow{13} \underset{\text{Hexagonal anhydrite}}{CaSO} \xrightarrow{200-} \underset{\text{Orthorhombic anhydrite}}{CaSO_4} \quad (3)$$

All products can be transformed to gypsum when mixed with water. However, the rate of gypsum forming may vary. For example, hexagonal anhydrite react rapidly whereas reaction of orthorhombic anhydrite and water may require an hour for forming gypsum, because the orthorhombic is more stable and complete packed crystal lattice (Anusavice *et al*., 2003).

2.2 Setting of calcium sulfate

The setting of calcium sulfate can be distinguished to two types including normal setting expansion that setting in the air whereas setting under water usually called hygroscopic setting expansion (Anusavice *et al*., 2003)

The setting time of calcium sulfate is influenced by the accelerators and retarders. The addition of inorganic salts, such as sodium chloride and potassium sulfate, to calcium sulfate accelerates the setting reaction by increasing the density of the seed crystal. However, in some report have not found this true (Gao *et al*., 2007). The retarders act by forming an absorbed layer on the hemihydrate to reduce its solubility and on the gypsum crystal present to inhibit growth. Organic materials, such as glue, gelatin and some gum, behave in this manner. Another type of retarder is salt that form a layer of calcium salt that less soluble than the sulfate. These may include borax, potassium citrate

and sodium chloride (20%). In small concentration, many inorganic salts act as accelerators, but when the concentration is increased, they can become retarders. Sodium chloride is an accelerator up to about 2% of the hemihydrates, but at a higher concentration, it acts as retarder. In the same way, sodium sulfate has its maximum acceleration effect at approximately 3-4%, at greater concentrations, it becomes a retarder (Anusavice *et al*., 2003).

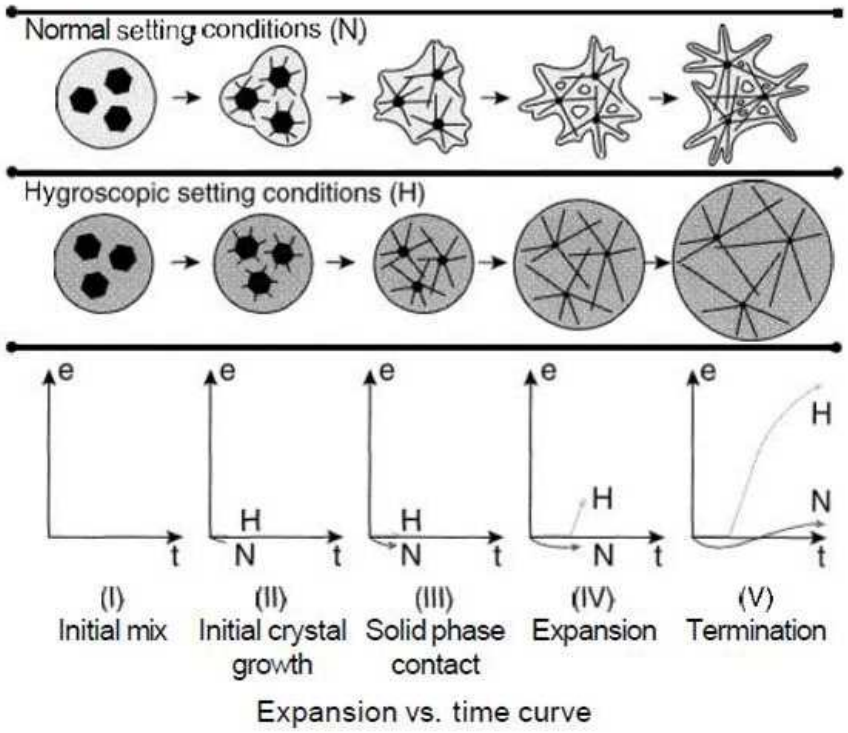

Figure 4 Diagram representation of the setting expansion of plaster. The above column, the crystal growth was inhibited by the lack of excess water. As shown in the below column, water added during setting provided more room for longer crystal growth. e = expansion, t = time, H = hygroscopic setting expansion, N = normal setting expansion.

Source: Mahler and Ady (1960)

The setting of calcium sulfate normally happen in the air. If the setting process occurs under the water, the setting expansion may be more than double in magnitude. The most well-accepted reason for increased expansion when the hemihydrates reacts under water is the additional crystal growth permitted by allowing the crystal to grow freely, rather than being constrained by the surface tension when the crystal forms in the air (Figure 4). In stage I, at the top of the figure, the initial mix is presented by the three round particles of hemihydrates surrounded by the water. In stage II, the reaction has started and the crystal of the dehydrate are beginning to form, On the left of diagram, the water around the particles is reduced by dehydration and these particles are drawn more closely together by the surface tension of the water. In the right-hand diagram, because the setting is taking place under the water, the water of hydration is replaced and the distance between the particles remains the same.

As the dehydrate crystals grow, they contact each other, and the setting expansion begins. As indicated in stage III, the water around the particles decreases in the example on the left. The particles with their attached crystal tend to be drawn together as before, but the contraction is opposed by the outward thrust of the growing crystals. On the other hand, the crystals in the diagram on the right are not inhibited, because the water is again replenished from the outside. In fact, the original particles are now separated further as the crystals grow, and the setting expansion is definitely evident.

In stage IV and V, the effect becomes more marked. The crystals that are inhibited on the left become intermeshed and entangled much sooner than those on the right, which grow much more freely during the early stages before the intermeshing finally prevents further expansion. Consequently, the observed setting expansion that occurs when the gypsum product sets under the water may be greater than that occurs during setting in the air (Mahler *et al*., 1960).

2.3 Bone defect augmentation

Calcium sulfate has been extensively used as bone substitute material for 90 years (Beuerlein *et al*., 2010). Multipurpose of calcium sulfate is the usage in clinic

including of bone substitute material and vehicle for antibiotic, pharmacologic agents and growth factors. Calcium sulfate can be used as bone filler, which has rapid and complete resorption without eliciting significantly inflammatory response. Although calcium sulfate has been studied for a long time in both *in vitro* and *in vivo* studies, however, many studies in the last decade years show that calcium is still interested in studying in a new form and a new preparation. The newer preparation include combination with other agents, such as chitosan (Cho *et al*., 2005; Cui *et al*., 2009), platelet-rich plasma (Intini *et al*., 2007) and bone morphogenetic protein-2 (BMP-2) (Cui *et al*., 2009), and new structure modification (Park *et al*., 2011). Most of studies show positive effect on bone healing in both *in vitro* studies (Lazary *et al*., 2007; Park *et al*., 2011; Sidqui *et al*., 1995) and *in vivo* studies (Ruhaimi *et al*., 2001; Cho *et al*., 2005; Intini *et al*., 2007; MacNeill *et al*., 1999; Pecora *et al*., 1997; Urban *et al*., 2004; Walsh *et al*., 2003). The mechanism of calcium sulfate enhancing bone regeneration has not been complete elucidate. Strocchi *et al.* (2002), created bone defects in the tibiae of rabbits, which were then filled with calcium sulfate granules or autogenous bone. Microvascular density was increased in calcium sulfate treated defects, suggesting a positive effect on angiogenesis (Strocchi *et al*., 2002). Walsh et al. filled femoral cancellous defects with calcium pellets and used immunohistochemistry to identify various growth factors *in situ* (Walsh *et al*., 2003). Increased concentration of bone morphogenetic protein (BMP-2), bone morphogenetic protein-7 (BMP-7), transforming growth factor-β (TGF-β) and platelet derived growth factor (PDGF) were observed, all of which played a role in connective tissue regeneration. From these both studies shown that calcium sulfate is not only inert filler but also plays more active role in osteogenesis. However, in some studies did not show positive effect on bone healing (Apaydin *et al*., 2004; Petruskevicius *et al*., 2002).

2.4 Drug delivery vehicle

In addition of calcium sulfate as space filler and barrier function, calcium sulfate has also been investigate as a local delivery vehicle for therapeutic agents, such as antibiotics, small molecule drugs, and growth factors (Thomas and Puleo, 2009). In 2007, Intini *et al.* have studied calcium sulfate and platelet-rich plasma as a novel

osteoinductive biomaterial and found that the calcium sulfate with platelet rich plasma can be used as osteoinductive material comparable to recombinant human bone morphogenetic protein (rh-BMP). In the same year Nyan *et al.* (2007) showed that calcium sulfate could be carrier of simvastatin. Simvastatis stimulated expression of BMP-2, for promoting bone regeneration in a critical-sized defect in the rat calvarium (Nyan *et al*., 2007). Calcium sulfate bead was widely studied in antibiotic release for osteomyelitis management in *in vitro* and *in vivo* studies. Many types of antibiotic have been studied with calcium sulfate bead such as gentamicin, vancomycin, teicoplanin, cephalexcin, tobramycin and enrofloxacin (Salgami *et al*., 2007; Tuzuner *et al*., 2007; Udomkusonsri *et al*., 2010; Wichelhaus *et al*., 2001). In addition, the calcium sulfate bead has been studied for improving facility of antibiotic releasing by incorporation with liposome (Hui *et al*., 2009) or coating with biodegradable polymer (Benoit *et al*., 1997).

3. Porosity

3.1 Scaffold for bone regeneration

Many researches of synthetic bone scaffolds were developed in last decade. Scaffolds have osteoconductive property, since new bone is deposited by creeping substitution from adjacent living bone. In addition to osteoconductive, scaffolds can serve as delivery vehicles for cytokines such as bone morphogenetic protein (BMPs), insulin-like growth factors (IGFs) and transforming growth factors (TGFs) that transform recruited precursor cells from the host into bone matrix producing cells, thus providing osteoinduction (Groeneveld *et al*., 1999). However, scaffolds for bone regeneration should meet criteria to serve this function, these including a high porosity and appropriate pore size, high surface area, biodegradability, mechanical integrity to maintain the pre-designed tissue structure, biocompatibility, positive interaction with cells, and also can be used as carrier for the delivery of growth and differentiation factors (Hutmacher *et al*., 2001).

3.2 Pore size and interconnectivity

Pores are necessary for bone tissue formation because they allow migration of endothelial cells: to promote osteoblasts or progenitor cells; to promote vascularisation of mesenchymal cells; or to facilitate osteoblast proliferation and differentiation. In addition, a porous surface improves mechanical stability and interlocking at the critical interface between the implant biomaterial and the surrounding natural bone.

The minimum pore size required to regenerate mineralized bone is generally considered to be 100 µm after the study of Hulbert et al. where calcium aluminate cylindrical pellets with 46% porosity were implanted in canine femur. Large pores (100-150 and 150-200 µm) showed substantial bone in-growth. Small pores (75-100 µm) resulted in in-growth of unmineralised osteoid tissue. Smaller pores (10-44 and 44-74 µm) were penetrating only by fibrous tissue (Hulbert *et al*., 1970). In addition a study of Bignon *et al*. (2003), show macroporosity (pore >50 µm) is thought to contribute to osteogenesis by facilitating cell and ion transport (Bignon *et al*., 2003). Studies suggest that microporosity (pores <20 µm) improves bone growth into scaffolds by increasing surface area for protein adsorption (Hing *et al*., 2005), increasing ionic solubility in the microenvironment (Habibovic *et al*., 2005; Le *et al*., 2005), and providing attachment points for osteoblasts (Bignon *et al*., 2003). Pore interconnectivity has been shown to positively influence bone deposition rate and depth of infiltration *in vitro* (Bignon *et al*., 2003) and *in vivo* (Hing *et al*., 2004). Regular interconnected pores provide spacing for the vasculature required for nourishing new bone and removing waste products (Hing *et al*., 2005; Jin *et al*., 2000; Kaito *et al*., 2005).

3.3 Pore and drug delivery

Porosity of the material is not only necessary for facilitation new bone formation in bone substitute materials but also promotion releasing of drug from the material (McLaren *et al*., 2004). The most common techniques used to create porosity in a biomaterial are salt leaching, gas foaming, phase separation, freeze-drying and sintering

depending on the material used to fabricate the scaffold (Karageorgiou *et al*., 2005). The method of leaching soluble particle is a simple technique for increasing porosity of the materials. The porosity can be effectively controlled by variation of the amount of leachable particles and the pore size of the porous structure can be adjusted independently of the porosity by using particles in difference sizes (Hou *et al*., 2003). Many studies of PMMA on increasing antibiotic releasing from the material were shown in different mixing method, add filler, difference of cement type, and ultrasound (Anagnostakos *et al*., 2009; Hou *et al*., 2003; McLaren *et al*., 2007; Rasyid *et al*., 2009; Shiramizu *et al*., 2008). In the report of van de Belt *et al*., they concluded that the kinetic of antibiotic releasing was initially controlled to some extent by surface phenomenon depending on the surface roughness of the PMMA, whereas the sustained releasing over a time span of several days depended on the penetration depth as determined by the bulk porosity of the cement (Figure 5) (Belt *et al*., 2000).

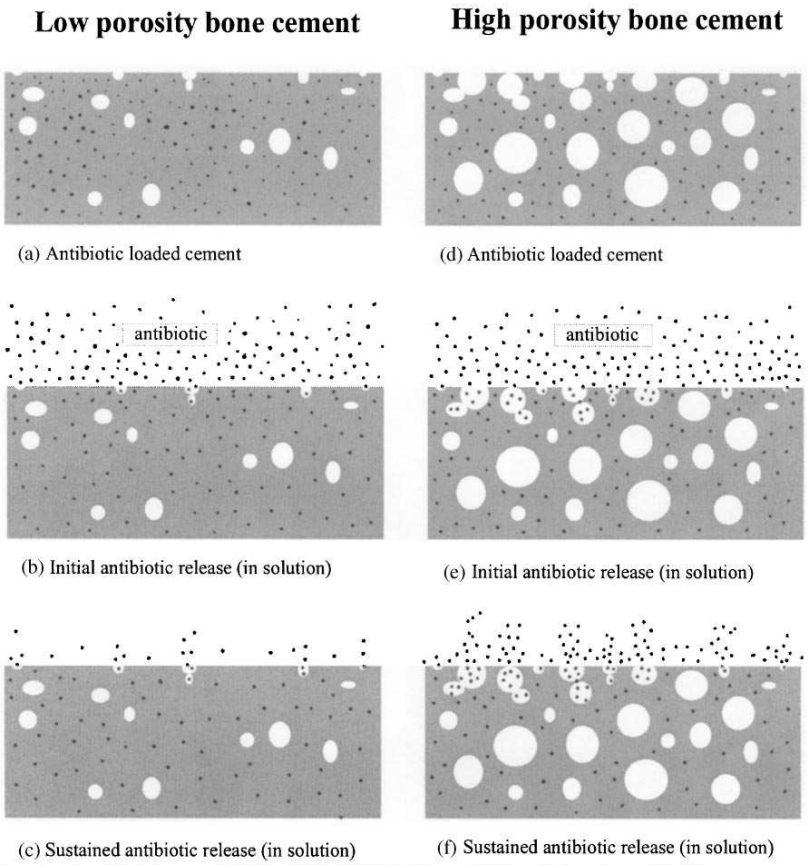

Figure 5 Proposed sequential steps in the releasing of gentamicin from a low-porosity (a-c) and high-porosity (d-f) bone cement. After a high initial release (b and e), there was a slow sustained release in time (c and f), which was depended on the penetration depth of the fluid through connection pores.

Source: Belt *et al*. (2000)

MATERIALS AND METHODS

1. Effect of porosity of calcium sulfate beads on ceftazidime elution and *in vitro* osteogenic properties

1.1 Calcium sulfate bead preparation

Calcium sulfate hemihydrates (Sigma, USA) and sodium chloride (Sigma, USA) were manually mixed together in varying weight ratios of 1:0 (control), 4:1, 2:1 and 1:1. Sterile distilled water was added to each mixture. The ratio of calcium sulfate hemihydrates and distilled water was 10:7 weight by volume (w/v). Thereafter, homogenous mixtures were poured into mold templates (6 mm in diameter × 4 mm height) and the beads were allowed to set at room temperature. The salt leaching process was conducted by immersing the beads in deionized water in an ultrasonic cleaner (JAC ultrasonic 4020P; KODO Technical Research Co. Ltd; Gyeonggi-Do, South Korea) for 5 cycles, for 30 minutes. All beads were dried in hot air oven at 60 °C overnight. The beads were weighted before and after salt leaching.

1.2 Physical characteristics of calcium sulfate beads

Each group of calcium sulfate beads was characterized by its total porosity, maximum compressive load, maximum compressive strength, water uptake and mass loss. The total porosity of the calcium sulfate beads in each group (10 samples per group) was determined by Archimedes's method (Bruckschen *et al*., 2005; Jones *et al*., 1993). Five beads from each group were tested for their maximum compressive load and maximum compressive strength with a universal testing machine (55R4502, S/N H3342; Instron; Canton, MA, USA) with a speed of 1 mm/min at 23 ºC and 50% relative humidity. For the water uptake measurement, 10 samples of calcium sulfate beads in each group were weighed after drying at 60ºC overnight and reweighed after immersion in sterile water (Baro *et al*., 2002). Ten samples of calcium sulfate beads in each group were

immersed in phosphate buffer saline (PBS) for 10 days during which time the PBS was changed every day. Then, all the beads were dried at 60 ºC overnight and weighed again to determine the mass loss. The mass loss was calculated as reported (Baro *et al*., 2002).

1.3 Preparation of ceftazidime beads

One gram of ceftazidime (CEF-4®, Siam Company, Thailand) was dissolved with 2 ml of sterile water (concentration 500 mg/ml). The calcium sulfate beads in each group were immersed in the ceftazidime solution overnight. All of beads were dried under a blower overnight.

1.4 Scanning electron microscopy

Calcium sulfate beads in each group (control, 4:1, 2:1, and 1:1) were examined using scanning electron microscopy (SEM) to determine the pore and crystal sizes of the calcium sulfate beads. The beads were coated with gold (IB-2, Eiko Engineer) and images of the outer surface and cross section were analyzed with a scanning electron microscope (JSM-5600LV; JEOL Ltd.; Tokyo, Japan) before and after adding ceftazidime.

1.5 *in vitro* Drug release study

Five antibiotic beads from each group were tested for drug elution using phosphate buffer saline (PBS) (pH 7.4) as the dissolution medium. The ceftazidime beads were immersed in 1 ml PBS at 37 ºC for 24 hours. The dissoluted PBS was collected and 1 ml fresh PBS was added every 24 hours for the 10 days of the experimental period. All dissolution samples were kept at -20 ºC until analysis. Eluted ceftazidime concentrations were determined by microbiological assay using *Micrococcus luteus* (ATCC 9341) as an indicator organism (Bennett *et al*., 1966; Joosten *et al*., 2005).

1.6 The *in vitro* Osteogenic properties testing with human osteoblast

The osteogenic properties of the calcium sulfate beads in ratios of 1:0 (control) and 1:1 were compared using human osteoblast (h-OBs). A calcium sulfate bead in each sample was loaded with 20 μl of h-OBs 2.5×10^5 cells/cm^3 and placed in a 24-well plate. Then, the 24-well plate was incubated in a CO_2 incubator at 37.0 ± 1.0 °C, with 5.0% CO_2 and 95 ± 5% humidity. The samples were analyzed on the first and seventh days after incubation to examine the viability and the morphology of the cell-seed specimen. The number of cells on the surface of the bead was observed by staining with acridine orange and examined using a fluorescent microscope (IX71; Olympus Corporation; Tokyo, Japan) on the first and the seventh day after incubation.

1.7 Data analysis

Relationships among the data in this study were studied by analysis of variance and comparisons between groups were investigated using the Tukey-Karmer multiple comparison test. All analyses were carried out using the statistical program NCSS 2007 (NCSS, LLC; Kaysville, UT, USA). Data were expressed as the mean ± SD. Statistical differences were tested at the $P < 0.05$ level.

2. Comparison of polymethylmethacrylate (PMMA) bead, native calcium sulfate (NCS) bead, and high porous calcium sulfate (HPCS) bead as gentamicin carriers and osteoblast attachment

2.1 Bead preparation

The highest porosity level of calcium sulfate ($CaSO_4.1/2H_2O$:NaCl = 1:1 w/w) bead was studied as high porous calcium sulfate bead (HPCS) to compare the gentamicin release characteristic among the groups of HPCS bead, native calcium sulfate

(NCS) ($CaSO_4.1/2H_2O$:NaCl = 1:0 w/w) bead, PMMA containing gentamicin, and PMMA coated with gentamicin.

The PMMA and calcium sulfate beads were categorized for elution test into four groups: gentamicin impregnated PMMA bead (GI-PMMA), gentamicin coated PMMA bead (G-PMMA), gentamicin coated native calcium sulfate bead (G-NCS), and gentamicin coated high porous calcium sulfate bead (G-HPCS).

Preparation of GI-PMMA beads: GENTAFIX3 (TEKNIMED S.A., France) consisted of 3.8% w/w gentamicin in polymethymethacrylate base. The bone cement powder was mixed with a liquid monomer according to company recommendation. The mixture was poured into the mold (diameter 5 mm × high 4 mm). For the complete polymerization, the PMMA was solidified at room temperature for 3 hours.

Preparation of G-PMMA beads: CEMFIX3 (TEKNIMED S.A., France) was a polymethymethacrylate bone cement without antibiotics. The PMMA was prepared according to company recommendation. After complete polymerization of PMMA, CEMFIX3 pellets were immersed in gentamicin solution, 40 mg/ml, (T.P.drug laboratory, Thailand) for 3 hours, then were dried under an air blower.

Preparation of G-NCS beads: Calcium sulfate hemihydrate ($CaSO_4$ ½ H_2O) (Sigma, USA) was used to prepare calcium sulfate beads. Ten grams of calcium sulfate hemihydrates were mixed with 7 ml distilled water. The homogenous mixture was poured into the mold (diameter 5 mm × high 4 mm) and the beads were set overnight at room temperature. After the settlement of calcium sulfate beads were achieved, these beads were submerged in gentamicin solution, 40mg/ml, (T.P.drug laboratory, Thailand) for 3 hours, then were dried under the blower.

Preparation of G-HPCS beads: Ten grams of calcium sulfate hemihydrates (Sigma, USA) were mixed with 10 g sodium chloride (Sigma, USA) and 7 ml distilled water. The homogenous mixture was poured into the mold until the beads set as G-NCS.

Sodium chloride was leached out of the calcium sulfate beads by using deionized water in an ultrasonic cleaner as described before.

2.2 Physical properties of antibiotic beads

Physical properties of GI-PMMA, G-PMMA, G-NCS, and G-HPCS beads were determined in aspect of weight (mg), total porosity (%), water uptake (%), and mass loss (%). The determination of total porosity of gentamicin beads was performed according to the Archimedes's principle of mass displacement (Bruckschen *et al*., 2005; Jones *et al*., 1993). Water uptake capacity of gentamicin beads was undertaken by weighing the gentamicin beads before and after the immersion in water (Baro *et al*., 2002). In addition, mass loss level was weighed before and after the gentamicin beads were bathed in PBS for 10 days (Baro *et al*., 2002).

2.3 Human's osteoblast attachment

Osteogenic compatibility of PMMA, NCS and HPCS beads were compared using human's osteoblasts (h-OBs) which were subcultured from primary human osteoblasts. Bead materials were loaded with 20 μL of h-OBs 2.5 $\times 10^5$ cells cm^{-3} in Dulbecco's Modified Eagle Medium (DMEM) complete medium (BioWhittaker, Lonza, USA) and placed in a 24-well plate. Then, that plate was incubated in CO_2 incubator at 37.0± 1.0 °C, 5.0% CO_2, and 95±5% humidity. The samples were analyzed in the first and the seventh days after the incubation for testing viability and morphology of cell-seed specimen.

The cell seed on the bead surface was observed by scanning electron microscopy (SEM). Samples were prepared according to standard method for SEM, including fixation, wash, dehydration by using critical point dryer (Bal-Tec CPD030, Bal-Tec Union Ltd., Liechtenstein), and gold coating with gold coater (JEOL JFC-1200, JEOL, Japan). The attachment of osteoblast on samples was observed by a scanning

electron microscope (HITACHI S-3400N, HITACHI, Japan) on the first and the seventh day after incubation.

2.4 Microstructure investigation

The gentamicin beads in each group were sampled randomly and analyzed with scanning electron microscope after drug loading to characterize the microstructure of bead and antibiotic housing. The beads were coated with gold (IB-2, Eiko Engineering,Co. Ltd., Japan) and analyzed with scanning electron microscope (JSM-5600LV, JEOL, Japan) operated by 10 kV at ×35, ×100, ×200 and ×500 from a cross-section and a surface view.

2.5 Determination of gentamicin elution test

Five beads in each group were immersed in phosphate buffer saline (PBS) (Sigma, USA). Each bead was incubated in 1 ml PBS, pH 7.4, at 37°C for 24 hours in a tube. The dissolution PBS was collected and 1 ml fresh PBS was added every 24 hour for 10 days through the experimental period. All dissolution samples were kept at -20°C until analysis and were tested within one week. Eluted gentamicin concentrations were determined by microbiological assay using *Bacillus subtilis* (ATCC 6633) as an indicator organism (Ficker *et al*., 1990).

2.6 Statistical analysis

All the analyses were carried out using NCSS 2007 (Kaysville, UT, USA). The concentration of gentamicin sulfate released from GI-PMMA, G-PMMA, G-NCS, and G-HPCS beads was analyzed by repeated ANOVA followed by a Tukey's multiple comparison test. Physical properties of the bead in each group were compared with one-way ANOVA and followed by a Turkey's multiple comparison test. Data was expressed as the mean ± standard deviation. Values with $P<0.05$ were considered statistical significant.

3. Efficiency of gentamicin impregnated polymethlymetacrylate (GI-PMMA) bead, gentamicin coated native calcium sulfate (G-NCS) bead and gentamicin coated high porous calcium sulfate (G-HPCS) bead on osteomyelitis management in a rat model

3.1 GI-PMMA, G-NCS and G-HPCS beads preparation

GI-PMMA: Commercial polymethymetacrylate (PMMA) with gentamicin sulfate 3.8% (GENTAFIX®3, Teknimed S.A., France) was used. Sterile powder and sterile liquid were mixed as the company recommendation. The mixture was poured into silicone cylinder mold (2×4 mm, diameter × height) and waited until the cement set. The PMMA beads were removed from the mold after setting.

G-NCS: Native calcium sulfate beads were prepared by mixing the calcium sulfate hemihydrates powder (Sigma, USA) with sterile distilled water in the ratio 10:7 w/v. The mixture was poured into silicone cylinder mold (2×4 mm, diameter x height) and waited until the calcium sulfate set. Calcium sulfate beads were immersed in gentamicin sulfate injection solution 40 mg/ml (T.P. drug laboratories, Thailand) for 5 minutes and dried under blower overnight.

G-HPCS: For preparation of high porous calcium sulfate beads, calcium sulfate hemihydrated and sodium chloride (sigma, USA) were weighted and manually mixed at ratio of 1:1 w/w. Sterile distilled water was added to the mixture in ratio 10:7 w/v of calcium sulfate hemihydrates and distilled water. After the mixture became homogenous slurry, it was poured into the cylinder mold. For salt leaching technique, the beads were placed with deionized water in an ultrasonic cleaner as described before. Calcium sulfate beads were immersed in gentamicin sulfate injection solution 40 mg/ml (T.P. drug laboratories, Thailand) for 5 minutes and dried under blower overnight. GI-PMMA, G-NCS and G-HPCS beads were sterilized with ethylene oxide before use.

3.2 Animals

Male wistar rats, approximately 3 months old, weight 250-300 g, were used in this study. All of rats were from the National Laboratory Animal Center, Mahidol University, Thailand. The rats were randomly selected for 4 groups, control (n=10), GI-PMMA bead (n=10), G-NCS (n=10) and G-HPCS (n=10). Rats were kept in individual cages with unlimited food and water. This study was approved by the Kasetsart university animal use committee.

3.3 Osteomyelitis model

Osteomyelitis was induced in left proximal tibia. The rats were anesthetized with pentobarbital (0.6 mg/kg) intraperitoneal injection. Left proximal tibias were prepared by hair shave, chlorhexidine scrub and alcohol as routine preoperative preparation. One centimeter skin incision was performed at craniomedian area of proximal tibia. Soft tissue and muscle were dissected through the bone. One millimeter hole at median cortex was be created with kirchner wire (K-wire) connecting to bone marrow. A K-wire (5.0×1.0 mm) coated with methicillin resistance *Staphylococcus aureus* (MRSA) (National institute of health, Department of medical sciences, Ministry of public health, Thailand) biofilm was inserted to marrow cavity. Five hundred microliters of 4.0×10^7 CFU/ml MRSA was injected to the bone marrow cavity. The fascia and soft tissue were closed with polyglyconate (Maxon®, 4-0). Skin was sutured with nylon (Difilon®, 4-0) interrupted suture. After inoculation, the left tibia was monitored for osteomyelitis by gross appearance and radiographic examination weekly until 3 weeks (Figure 6).

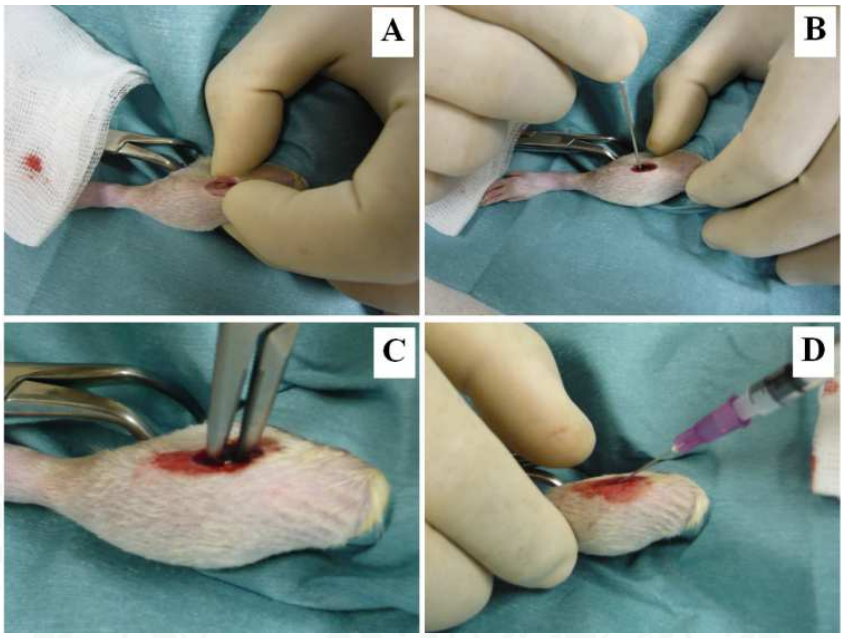

Figure 6 Osteomyelitis induction procedures at the left tibia. craniomedian at proximal part of tibia was opened (A), the median cortex was drilled by the 18 gauge needle (B), the Kirchner wire was inserted to the rat's tibia by needle holder (C) and MRSA solution was injected to the marrow cavity (D).

3.4 Surgical procedure

After 3 weeks post-inoculation, the rats were anesthetized with pentobarbital (0.6 mg/kg) intraperitoneal injection. Left proximal tibia was prepared by hair shave, chlorhexidine scrub and alcohol as routine preoperative preparation. Soft tissue and abscess capsule were removed and irrigated with 0.9% saline solution. Kirchner wire was removed from bone marrow cavity. Wound was sutured in control group without any additional treatment. In GI-PMMA group, two GI-PMMA beads were implanted to the marrow cavity of left proximal tibia. As GI-PMMA group, the G-NCS and G-HPCS beads were implanted to the marrow cavity of left proximal tibia. The soft tissue and skin were closed routinely.

3.5 Infection signs

The infection signs and white blood cell count were monitored weekly for 3 weeks. The infection signs score were from 0-4 (0 = no evidence of erythema, no pain and no swelling at infected site, 1 = erythema without abscess, no pain and mild swelling at infected site, 2 = erythema with swelling of the infected site, pain, 3 = purulent exudate, pain and swelling at infected site and 4 = purulent exudate, severe pain and tibia swelling). The clinical sign score was modified from categorized of Rissing, J.P. (Rissing *et al*., 1985)

3.6 White blood cell count

The blood samples (0.5 ml) were collected from tail vein in EDTA container before MRSA inoculation at the day of treatment and every week post treatment until 6 weeks. Total white blood cell count was determined by automatic white blood cell counting machine (CELL-DYN®3700, Abbott laboratories, Illinois, USA). The cell was presented in total number of white blood cell$\times 10^3/\mu l$.

3.7 Radiographic examination

Rats in each group were taken for radiographic examination (40 kV, 10 mAs, 100 cm) in anterioposterior and mediolateral views before and after tibia infected with MRSA weekly until the end of the study. The radiographic results were assessed for basis of periosteal elevation (PE), architectural deformation (AD), widening of the bone shaft (WBS), new bone formation (NMF), percentage of radiolucent area (PRA) and soft tissue deformation (STD). Each parameter will be scored on a 5 points scale (0-4) and the total summation of respective radiological parameters were calculated as the total radiological score (total RS) (Smeltzer *et al*., 1997).

3.8 Bone culture

The whole right tibias were collected with sterile procedure after rat euthanasia. All soft tissues were removed from the tibia samples. The tibia samples were weighted and pulverized with mortar under sterile condition. One milliliter of sterile normal saline solution was added to the bone samples tube and quantitatively culture by ten consecutive 1:10 dilution in sterile normal saline. A 0.1 ml aliquot of each dilution was plated onto Mueller Hinton agar (Difco, USA) and incubated in 37 °C for 18-24 hours. The colonies on the surface of agar plate were counted for calculating the colony forming unit (CFU) per weight (gram) of bone. Bacterial growth was expressed as log10 CFU/g tissue.

3.9 Histological examination

After euthanizing the rats with over dose pentobarbital, tibias were stored in 10% neutral formalin more than 24 hours. The samples were decalcified with 10% aqueous EDTA for a month and examined by a routine tissue processing for light microscopic procedure. The samples were stained with hematoxylin and eosin (H&E) for examine the cell types and Masson's trichrome for examine the bone collagen. Histopathological results were evaluated according the parameters including 1. Abscess formation, 2. Sequestrum formation, 3. Enlargement of corticalis, 4. Destruction of corticalis, 5. General impression. The parameter 1-4 were scored with 0 (absent) or 1 (present). Parameter 5 was scored from 0 (absent), 1 (mild), to 2 (severe) for each ROI. (Lucke *et al*., 2003).

3.10 Data analysis

The clinical sign score, white blood cell count, radiographic score and histopathological score were analyzed with Kruskal-Wallis One-Way ANOVA. Data was expressed as the mean ± standard deviation. Statistical difference was accepted with a $P<0.05$ level.

RESULTS

1. Effect of Porosity of Calcium Sulfate Beads on Ceftazidime Elution and *in vitro* Osteogenic Properties

1.1 Calcium sulfate beads

A salt leaching process was applied in the present study to produce calcium sulfate beads with a wide range of porosities. The outer surfaces of the calcium sulfate beads are shown in Figure 8. The highest surface porosity was identified grossly in the 1:1 group (Figure 7).

Figure 7 Calcium sulfate beads of various porosities after salt leaching technique: Top view (A); and Side view (B) after mixing calcium sulfate hemihydrates with sodium chloride at ratios of 1:0 (control), 4:1, 2:1 and 1:1 from left to right, respectively.

1.2 Characteristics of calcium sulfate beads

The total porosity is shown in Table 1. In the control group, the total porosity was 19.40 ± 3.87%. After salt leaching, the total porosity of the 4:1, 2:1 and 1:1 groups was 22.76 ± 5.21, 27.53 ± 3.05 and 48.08 ± 3.98%, respectively. The beads in the control group had less porosity compared with others and beads in the 1:1 group had the highest porosity. Although the porosity of the beads in the 2:1 group was slightly higher than the beads in the 4:1 group, there was no statistically significant difference between them.

The highest maximum compressive load and maximum compressive strength were found in the control group with values of 593.32 ± 56.77 N and 22.24 ± 1.34 MPa, respectively. Salt leaching led to a significant decrease in both the maximum compressive load and maximum compressive strength in the 4:1, 2:1 and 1:1 groups of beads, respectively (Table 1).

The percentage of water uptake of calcium sulfate beads in each group is shown in Table 1. The capacity for water uptake was found highest in the 1:1 group (46.64 ± 4.42%) and lowest in the control group (19.69 ± 1.21%). After the calcium sulfate beads were immersed in PBS for 10 days, the control beads presented the lowest percentage of mass loss (3.40 ± 0.68%). Salt leaching positively increased the percentage of mass loss in the 4:1, 2:1 and 1:1 groups of beads with values of 6.11 ± 0.29, 10.79 ± 0.92 and 11.90 ± 1.37%, respectively.

Table 1 Physical characteristics of calcium sulfate beads.

Group	Characteristics					
	Total porosity (%)	Maximum compressive load (N)	Maximum compressive strength (MPa)	Water uptake (%)	Mass loss (%)	Weight (mg)
Control	19.40±3.8[a]	593.32 ± 56.77[a]	22.24 ± 1.34[a]	19.69 ± 1.21[a]	3.40 ± 0.68[a]	161.98±3.9[a]
4:1	22.76±5.2[ab]	120.74 ± 13.79[b]	4.75 ± 0.50[b]	22.92 ± 1.19[b]	6.11 ± 0.29[b]	145.54±7.7[b]
2:1	27.53±3.0[b]	66.94 ± 4.89[c]	2.69 ± 0.19[c]	28.92 ±1.82[c]	10.79 ±0.92[c]	121.76±6.8[c]
1:1	48.08±3.9[c]	62.23 ± 6.45[c]	2.48±0.25[c]	46.64 ± 4.42[d]	11.90 ±1.37[c]	83.34±2.03[d]

[a,b,c] = Mean ± SD in each column with different superscript letters are significantly different ($P < 0.05$).

1.3 Scanning electron microscopy

Scanning electron microscopy was used to study the microstructure of the calcium sulfate beads in each group. The cross section and surface views of the CS beads before and after adding ceftazidime were observed (Figure 8). In the cross section view, the average calcium sulfate crystal size from the control group (1.46 ± 0.31 µm) was significantly smaller than for the 4:1, 2:1 and 1:1 groups (12.60 ± 1.97, 13.47 ± 1.99 and 13.47 ± 2.03 µm, respectively) as shown in Figure 9. Interestingly, the average calcium sulfate crystal width on the surface view varied between 8 and 20 µm and was not different among the groups. Furthermore, the average pore size in the control group (1.49 ± 0.67 µm) was smaller than in the other groups. Small and large pores were found after salt leaching in the 4:1, 2:1 and 1:1 groups sized 10.98 ± 3.18 µm and 359.98 ± 55.31 µm, respectively (Figures 8A–8D). After adding ceftazidime, the CS crystals were coated with a thin layer of ceftazidime. In addition, ceftazidime crystals

were found in the small holes (2–20 µm), while there were no ceftazidime crystals in the large holes in all groups (Figures 8E–8H).

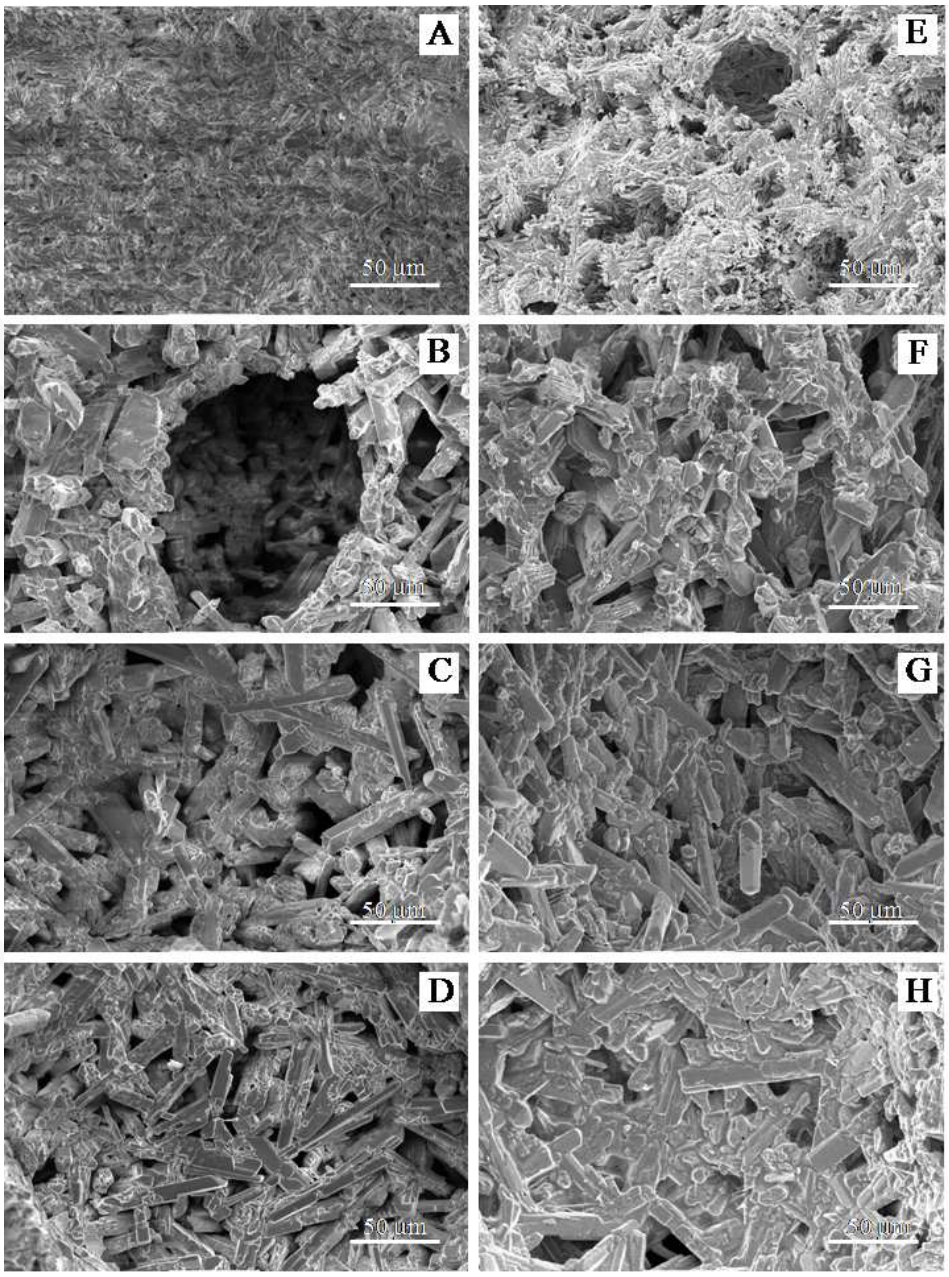

Figure 8 Cross sectional views of various calcium sulfate beads: Control (A, E), 4:1 (B, F), 2:1 (C, G) and 1:1 (D, H) groups compared before (A–D) and after (E–H) adding ceftazidime. (500×)

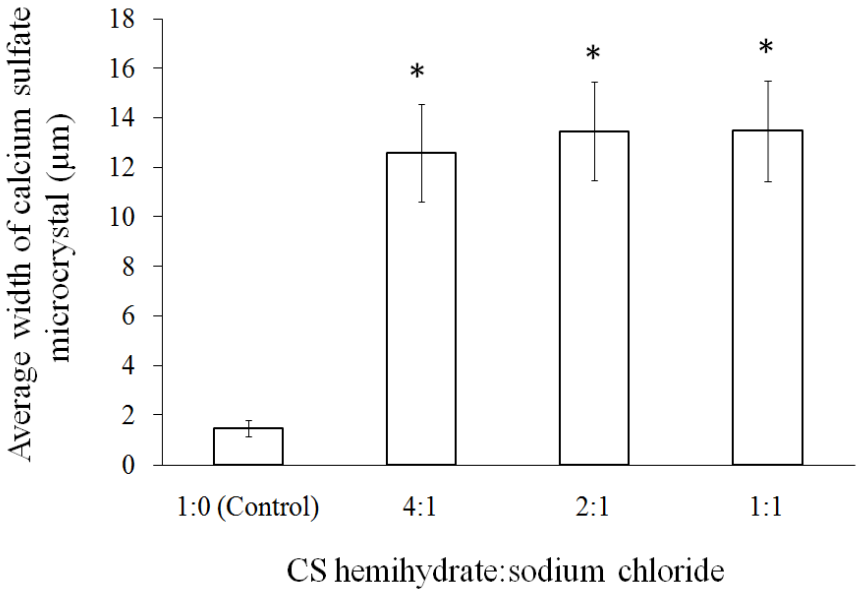

Figure 9 Comparison of average calcium sulfate (CS) crystal width between groups. (* = $P < 0.05$ compared to control group).

1.4 Elution of ceftazidime

The amount of eluted ceftazidime from the ceftazidime-impregnated calcium sulfate beads was determined by microbiological assay. The eluted ceftazidime was significantly highest ($P < 0.0001$) on the first day in all group, however there was no difference in eluted ceftazidime among groups (Figure 10). Released ceftazidime from the calcium sulfate beads could be detected for 6 days in the control group, while in the 4:1 and 2:1 groups, ceftazidime could be detected for 5 days and in the 1:1 group only for 4 days (Figure 10). The concentration of ceftazidime that *M. luteus* can be detected was limited (low of detection = 8 µg/ml).

The accumulative amounts of eluted ceftazidime from the calcium sulfate beads in the control, 4:1, 2:1 and 1:1 groups were 9.55 ± 1.35, 5.80 ± 2.30, 6.55 ± 1.73 and 8.91 ± 2.66 mg, respectively. In addition, the total amount of eluted ceftazidime per weight of calcium sulfate bead in the 1:1 group (160.63 ± 46.84 mg per gram) was the highest followed by the 2:1, 4:1 and control groups with 89.39 ± 24.60, 79.00 ± 16.39

and 59.10 ± 9.48, respectively (Figure 11). Furthermore, the total amount of ceftazidime released in milligrams from the calcium sulfate beads per weight of calcium sulfate bead in grams and the total porosity (%) had a positive correlation with an R value of 0.8152 ($P < 0.001$) as shown in Figure 12.

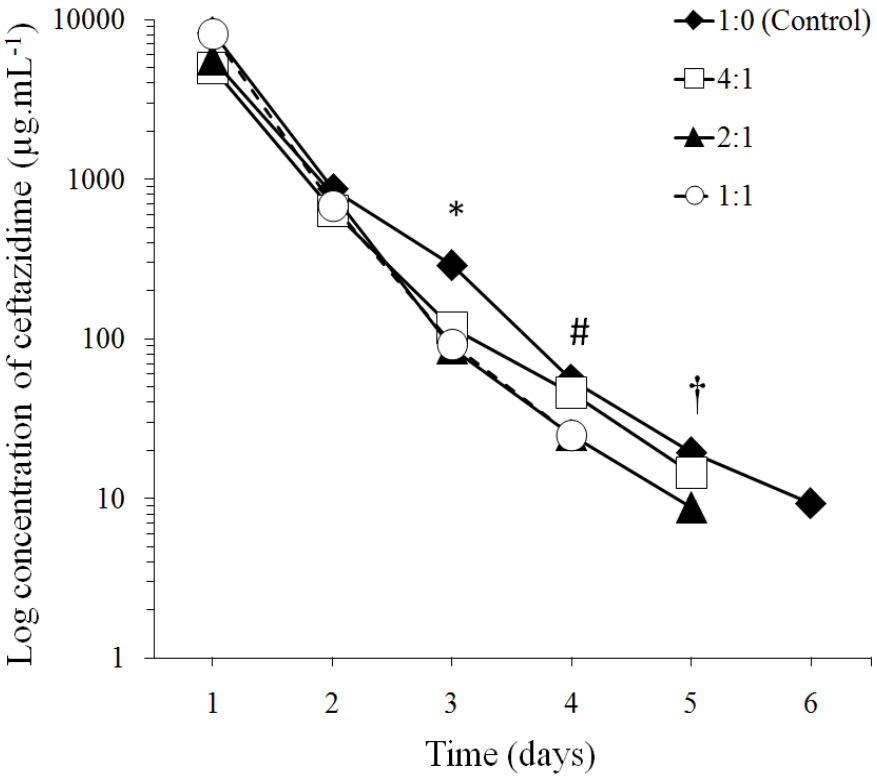

Figure 10 Concentration of ceftazidime released from calcium sulfate beads each day. (* = $P < 0.05$ comparison between control and 4:1, 2:1 or 1:1; # = $P < 0.05$ comparison between control and 2:1 or 1:1; † = $P < 0.05$ comparison between control and 2:1).

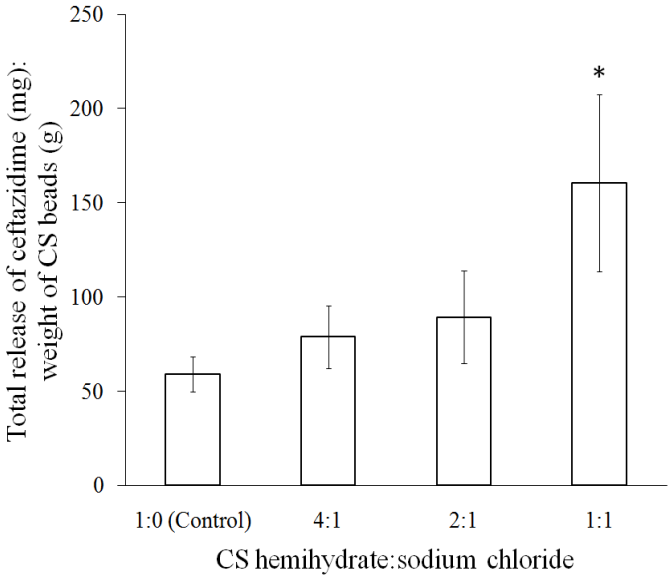

Figure 11 Ratio of total release of ceftazidime to the weight of calcium sulfate (CS) beads in each group. Data are presented as mean ± SD. (* = significant at $P < 0.05$ level compared to other groups).

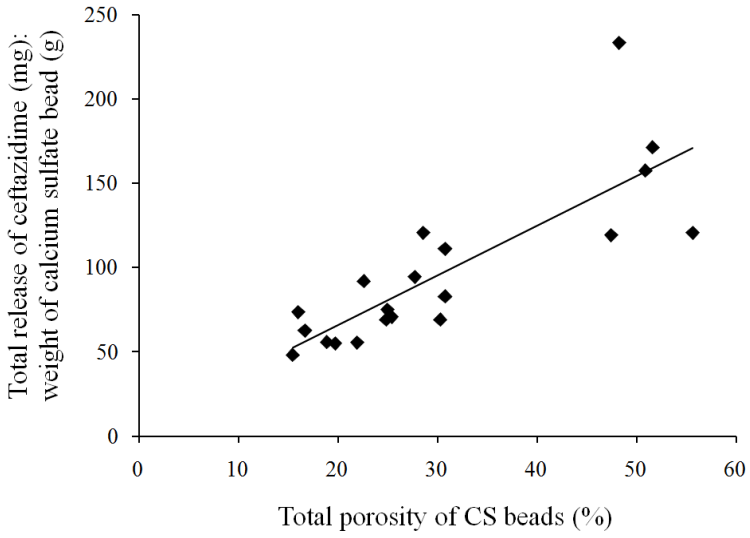

Figure 12 Ratio of total release of ceftazidime to the weight of calcium sulfate (CS) beads showing a positive correlation with total porosity of CS beads *P<0.001* (R = 0.8152).

1.5 *in vitro* Osteogenic testing with human osteoblasts

Acridine orange staining was used to examine the human osteoblast (h-OBs) seed in the control and 1:1 beads. The h-OBs could survive and proliferate on the surface of the control and 1:1 beads on the first day and the seventh day after incubation. Interestingly, fluorescence analysis determined that the number of h-OBs cells in the high porosity calcium sulfate beads (1:1 group) was significantly ($P < 0.05$) higher than in the control beads on the first day (1.98 fold increases) and on the seventh day (1.59 fold increase) (Figure 13).

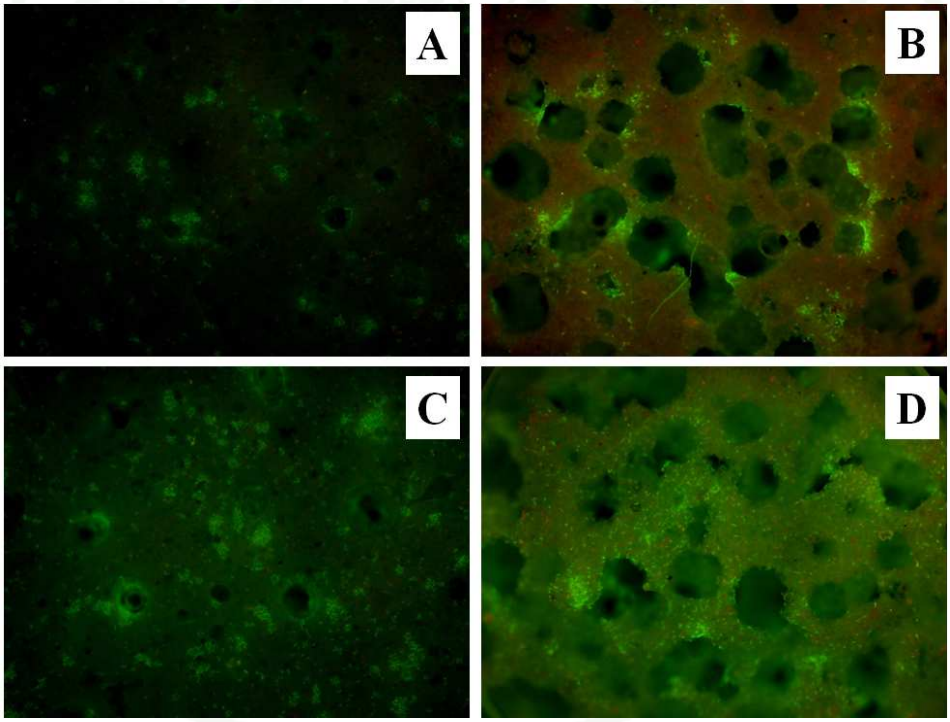

Figure 13 Acridine orange staining of human osteoblasts (h-OB) on calcium sulfate beads (×40): (A) Calcium sulfate bead (control) after 24 hours of co-cultivation with h-OB; (B) calcium sulfate bead (1:1) after 24 hours of co-cultivation with h-OB; (C) calcium sulfate bead (control) after 7 days of co-cultivation with h-OB; and (D) calcium sulfate bead (1:1) after 7 days co-cultivation with h-OB.

2. Comparison of polymethylmethacrylate (PMMA) bead, native calcium sulfate (NCS) bead, and high porous calcium sulfate (HPCS) bead as gentamicin carriers and osteoblast attachment

2.1 Antibiotic beads characteristics

Gross appearances of GI-PMMA, G-PMMA, G-NCS and G-HPCS beads are shown in Figure 14. The GI-PMMA and G-PMMA beads had no visible pores on the surface, while G-NCS beads had a small number of visible pores. Interestingly, G-HPCS beads had numerous visible pores on the bead surface. Physical properties of gentamicin beads, including weight (mg), porosity (%), water uptake (%), and mass loss (%) are shown in Table 2.

Figure 14 The beads were presented in each group in top and side views. Beads were arranged from left to right in the following order: GI-PMMA, G-PMMA, G-NCS and G-HPCS, respectively. GI-PMMA and G-PMMA beads had no visible pores on the surface while G-NCS beads had little pore numbers on the surface. Numerous visible pores were found on the surface of G-HPCS in both top and side views.

Table 2 Physical properties of antibiotic beads including weight (mg), porosity (%), water uptake (%), and mass loss (%) in GI-PMMA, G-PMMA, G-NCS, and G-HPCS beads.

Group	Weight (mg)	Porosity (%)	Water uptake (%)	Mass loss (%)
GI-PMMA	119.38±7.45[a]	2.10±2.82[a]	8.65±1.88[a]	1.50±0.25[a]
G-PMMA	117.93±8.36[a]	2.89±3.37[a]	7.56±3.16[a]	0.78±0.47[a]
G-NCS	163.08±5.73[b]	25.71±5.10[b]	27.17±2.42[b]	5.73±0.48[b]
G-HPCS	84.92±6.38[c]	42.32±4.57[c]	51.15±4.66[c]	9.19±1.52[c]

[a,b,c] The different superscript within column indicate significant difference ($P < 0.05$)

2.2 Human's osteoblast attachment

Since a different concentrations of gentamicin were released from each bead and might has had effect on cellular growth and proliferation, GI-PMMA, G-PMMA, G-NCS, and G-HPCS were not used for an osteoblast attachment test. Three types of bead materials were used, including PMMA beads, NCS beads and HPCS beads. Scanning electron microscopic images of material surface showed the intact h-OBs cells with normal morphology and extending filopodia (Figure 15) in which indicated the survival of h-OBs on PMMA, NCS, and HPCS bead surfaces. Interestingly, scanning electron microscopic pictures displayed that the h-OBs numbers weresignificantly increased in HPCS beads compared with that in NCS beads and in PMMA beads after cell culture for 7 days.

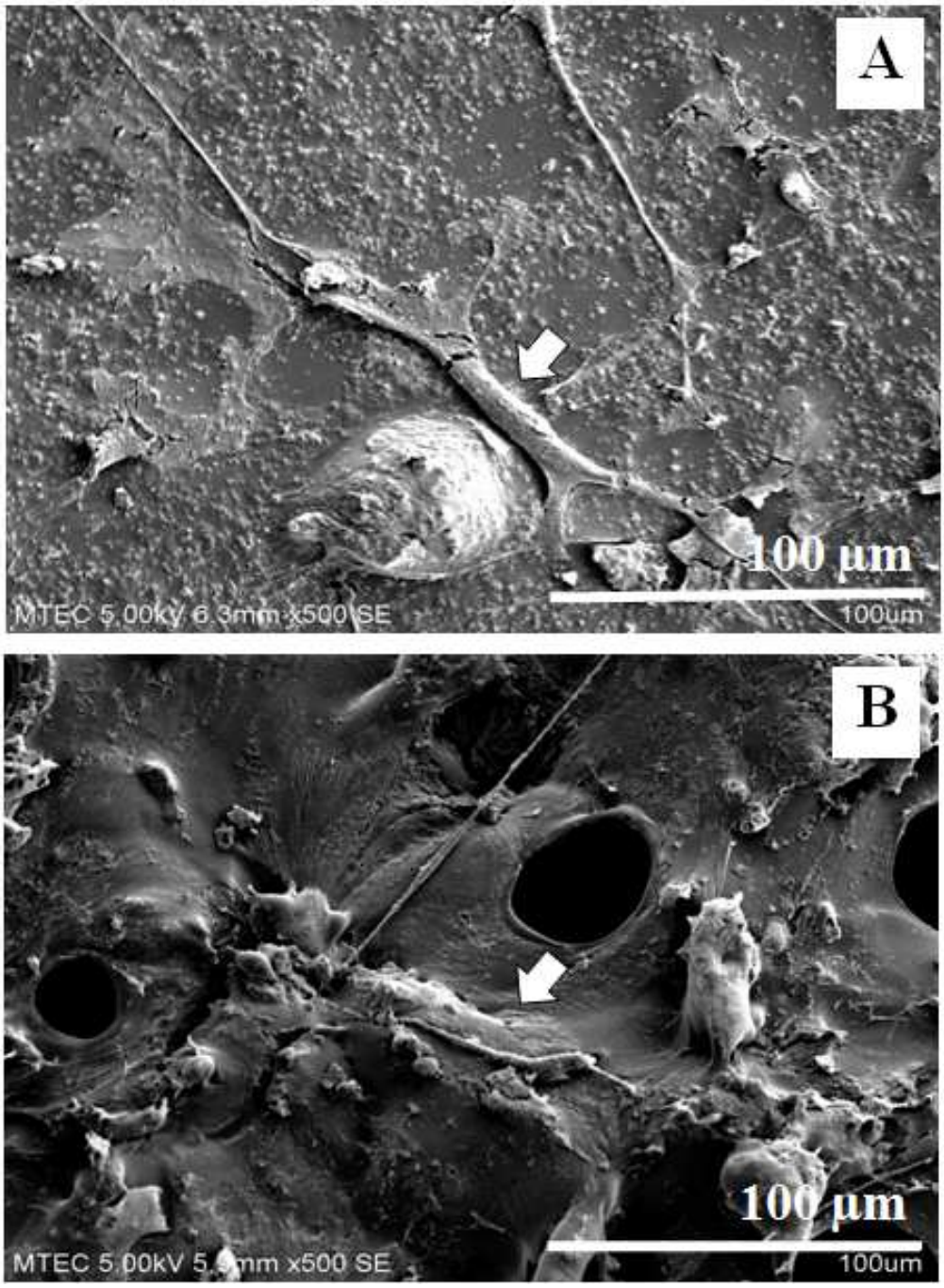

Figure 15 The human osteoblast (h-OBs) (white arrows) attached on the surface of the bead. A = PMMA Day 1, B= PMMA Day 7.

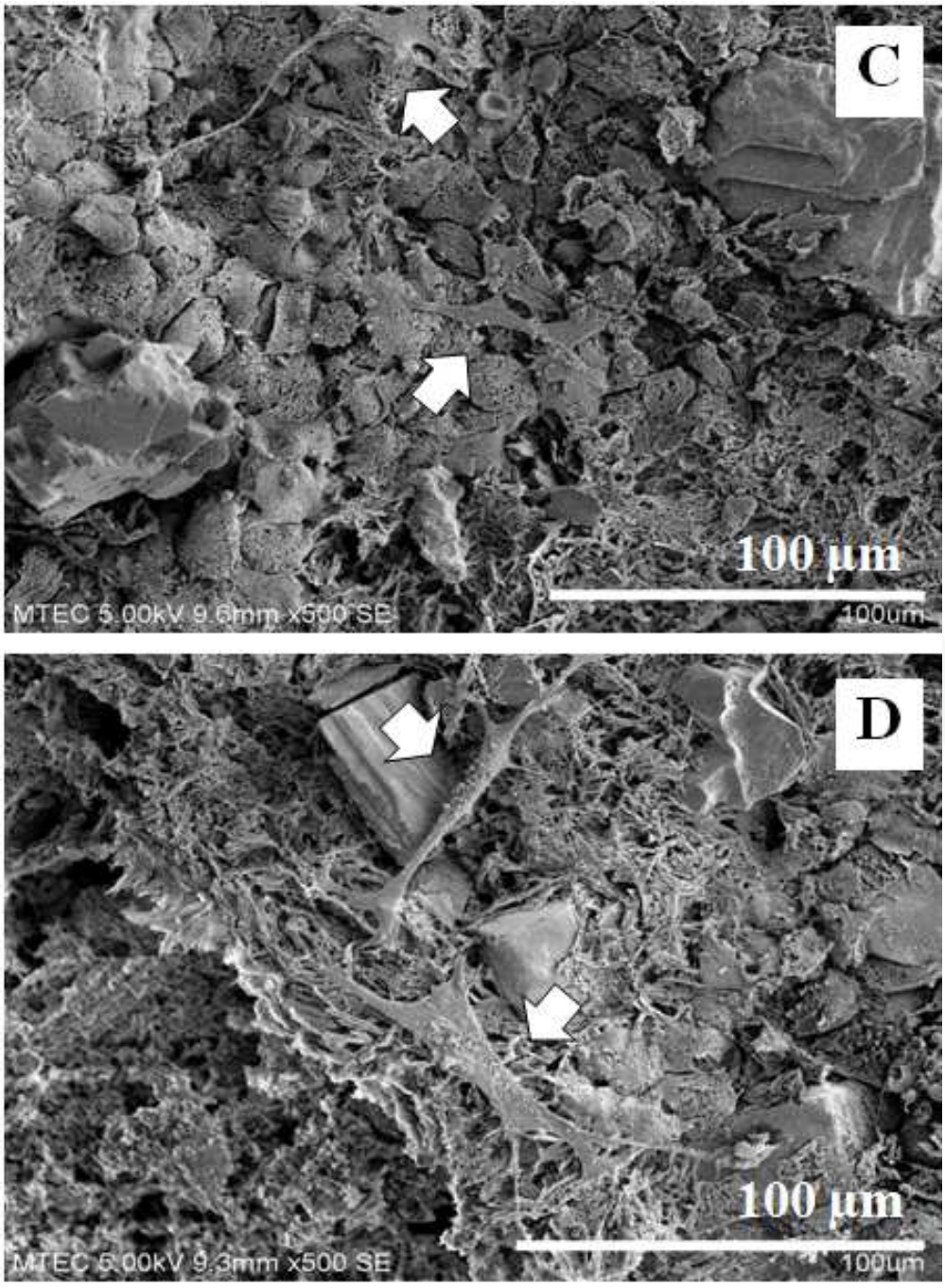

Figure 15 (continued) The human osteoblast (h-OBs) (white arrows) attached on the surface of the bead. C = NCS Day 1, D = NCS Day 7.

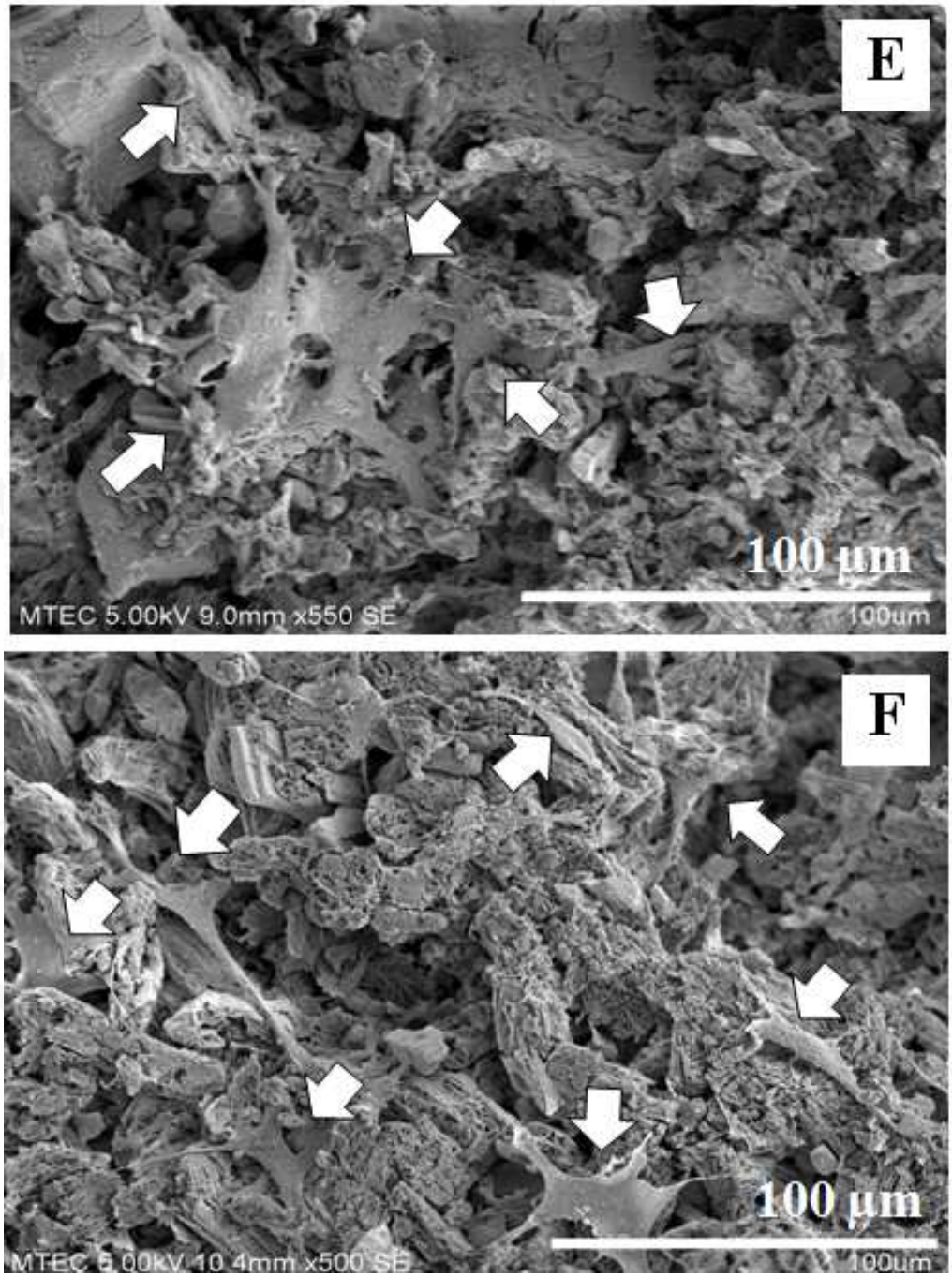

Figure 15 (continued) The human osteoblast (h-OBs) (white arrows) attached on the surface of the bead. E = HPCS Day 1, F= HPCS Day 7.

2.3 Microstructure observation

According to GI-PMMA, G-PMMA, G-NCS, and G-HPCS beads, all consisted of different microstructures. GI-PMMA and G-PMMA beads had no crystal structures and fewer pores, while G-NCS and G-HPCS beads had crystal structures and numerous pores (Figure 16). Surface of GI-PMMA bead was rougher than such of G-PMMA bead. The cross sectional view of GI-PMMA and G-PMMA beads showed the cracks on the rough surface, but gentamicin particle was not observed in both groups. Furthermore, fewer holes were noticed on both surface and the cross-section views in both GI-PMMA and G-PMMA beads.

The microstructure of G-NCS and G-HPCS beads was different in terms of porosity and crystal size on both surface and cross sectional views. The average diameters of calcium sulfate crystals of G-NCS and G-HPCS beads were 1.15±0.23 μm and 10.42±2.04 μm, respectively, whereas the average pore sizes of G-NCS and G-HPCS beads were 1.59±0.31 μm and 22.37±6.48 μm, respectively. Not only in the G-HPCS bead, but macropores were also found in G-NCS bead. G-HPCS bead consisted of numerous macropores (average size = 385.44±101.97 μm) in both cross sectional and surface views, while little macropores were shown in G-NCS bead. In addition, both surface and cross sectional views, the crystal structure of calcium sulfate was coated with gentamicin sulfate, while it was not observed in the PMMA beads.

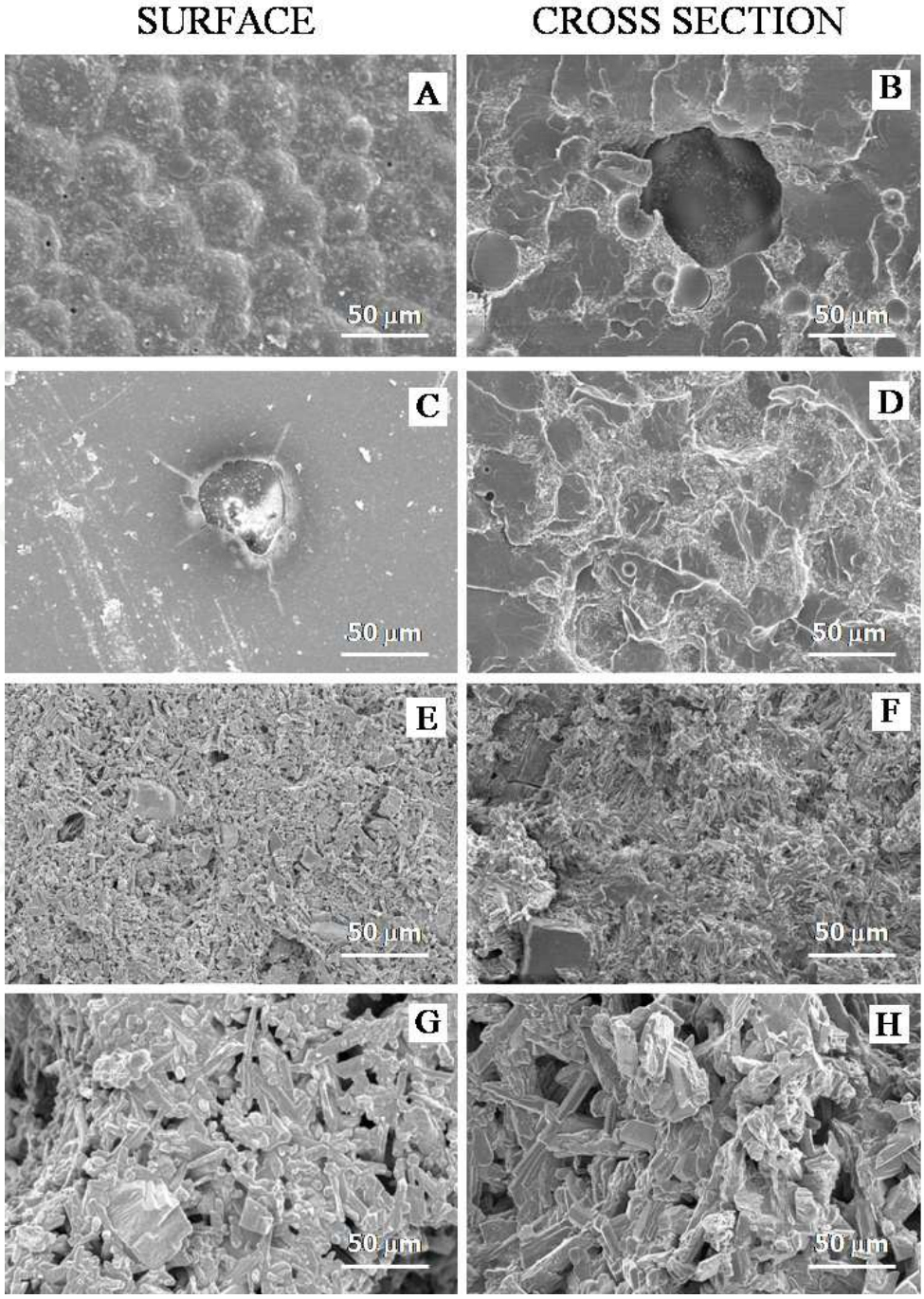

Figure 16 Scanning electron microscope micrograph presented the microstructure of gentamicin bead including GI-PMMA (A,B), G-PMMA (C,D), G-NCS (E,F) and G-HPCS (G,H). Left column is a surface view. Right column is a cross-sectional view. (magnification = 500×).

2.4 Antibiotic dissolution

Elution characteristics of GI-PMMA, G-PMMA, G-NCS, and G-HPCS beads were significantly different from one another in terms of concentrations of each day (Table 3). The total amount of gentamicin released from GI-PMMA and G-PMMA beads was 716.87±272.72 and 1381.64±486.38 µg/ ml, respectively, while that in G-NCS and G-HPCS beads was 5003.45±517.27 and 4901.50±1072.69 µg/ml, respectively, during 10-dayexperimental period. Gentamicin sulfate could be detected only for 4 days in G-PMMA bead, while GI-PMMA bead could provide gentamicin sulfate until the end of the experiment, similar to G-NCS and G-HPCS beads. The concentration of gentamicin that *B.subtilis* can be detected was limited (low of detection = 0.1 µg/ml). Concentrations of gentamicin sulfate released from G-HPCS bead were higher than from GI-PMMA and from G-PMMA beads in the first 5 days, they, thereafter, decreased to the same level as of GI-PMMA bead in the next 5 days. The gentamicin sulfate released from all types of beads in current study was found mostly within the first day of the experiment. As these can be seen that the percentage of gentamicin released from of GI-PMMA, G-PMMA, G-NCS, and G-HPCS beads of 13.05±7.21%, 95.44±1.07%, 52.36±6.41%, and 81.98 ±1.65%, respectively (Table 4). The total quantity of gentamicin sulfate in the eluted solution from GI-PMMA and G-PMMA beads was significantly lower than that released from G-NCS and G-HPCS beads (Table 3).

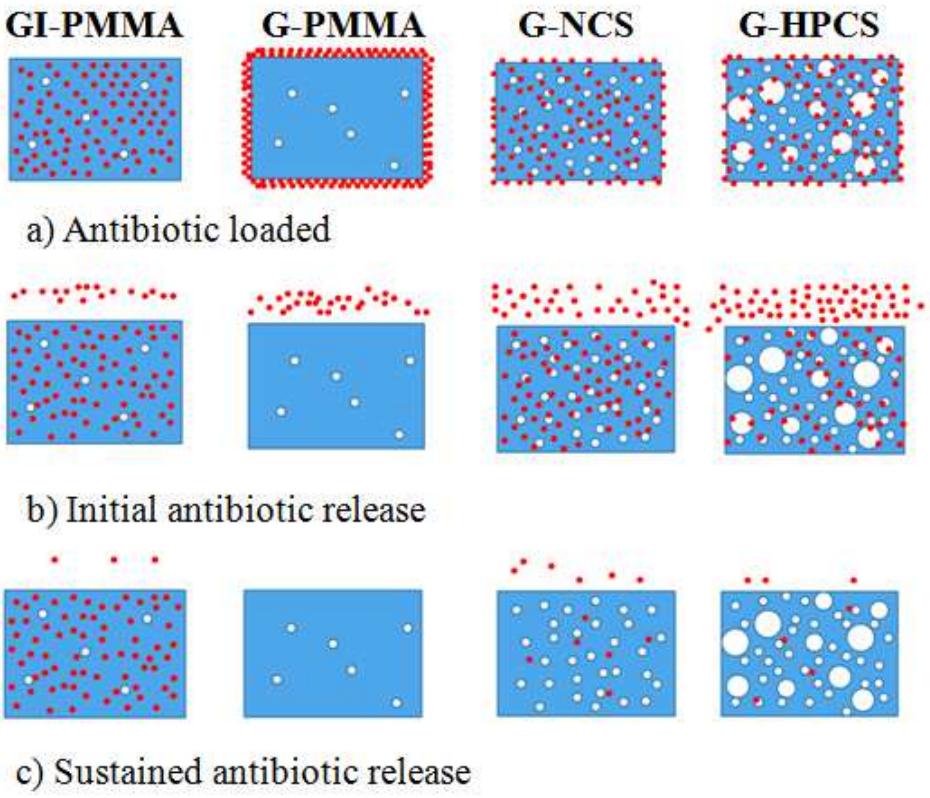

Figure 17 Phase of antibiotic releasing from GI-PMMA, G-PMMA, G-NCS, and G-HPCS. High antibiotic release is shown in initial phase and low antibiotic release is shown in sustained phase.

Table 3 Concentration of gentamicin sulfate (µg/ml) released from GI-PMMA, G-PMMA, G-NCS and G-HPCS beads during 10 days-experimental periods.

Day	Concentrations of gentamicin sulfate (µg/ml)			
	GI-PMMA	G-PMMA	G-NCS	G-HPCS
1	571.48±279.88[a]	1318.88±465.45[b]	2640.54±470.28[c]	4016.43±846.03[c]
2	66.53±18.07[a]	55.38±25.65[a]	1058.85±160.67[b]	624.56±247.94[b]
3	26.69±4.81[a]	6.77±1.91[b]	852.76±204.23[c]	159.05±25.84[d]
4	16.28±3.51[a]	0.61±0.33[b]	238.21±36.87[c]	48.03±13.96[d]
5	9.55±3.72[a]	UD	102.87±64.40[c]	23.32±7.11[b]
6	8.60±1.87[a]	UD	52.05±15.97[b]	12.21±3.35[a]
7	6.55±1.82[a]	UD	27.44±8.22[b]	7.34±1.86[a]
8	3.83±1.48[a]	UD	13.99±2.32[b]	4.93±1.15[a]
9	4.27±1.67[a]	UD	10.65±2.67[b]	2.93±1.03[a]
10	3.11±0.75[a]	UD	6.10±1.43[b]	2.70±0.42[a]
Total	716.87±272.72[a]	1381.64±486.38[a]	5003.45±517.27[b]	4901.50±1072.69[b]

[a,b,c,d] The different letters within row indicate significant difference within day ($P < 0.05$).

UD = undetectable

Table 4 Percentage of gentamicin release in each day from GI-PMMA, G-PMMA, G-NCS and G-HPCS beads.

Day	GI-PMMA	G-PMMA	G-NCS	G-HPCS
1	13.05±7.21[a]	95.44±1.07[b]	52.36±6.41[c]	81.98±1.65[d]
2	1.49±0.42[a]	3.99±1.03[a]	21.19±3.44[b]	12.27±2.91[b]
3	0.60±0.15[a]	0.52±0.15[a]	16.86±3.40[b]	3.46±1.30[a]
4	0.36±0.07[ab]	0.05±0.02[a]	4.74±0.66[c]	1.02±0.36[b]
5	0.22±0.10[a]	UD	2.08±1.42[b]	0.49±0.17[a]
6	0.19±0.05[a]	UD	1.05±0.38[b]	0.26±0.10[a]
7	0.15±0.05[a]	UD	0.55±0.19[b]	0.15±0.05[a]
8	0.09±0.04[a]	UD	0.28±0.07[b]	0.10±0.04[a]
9	0.09±0.04[a]	UD	0.21±0.06[b]	0.06±0.02[a]
10	0.07±0.02[a]	UD	0.12±0.04[b]	0.06±0.02[a]
% total release	16.32±7.22[a]	100±0.00[b]	99.44±0.22[b]	99.86±0.04[b]
Total (mg/bead)	4.48±0.31[a]	1.38±0.49[b]	5.03±0.52[a]	4.91±1.07[a]

[a,b,c,d] The different letters within row indicate significant difference within day ($p < 0.05$).

UD = undetectable

3. Efficiency of gentamicin impregnated polymethlymetacrylate (GI-PMMA) bead, gentamicin coated native calcium sulfate (G-NCS) bead and gentamicin coated high porous calcium sulfate (G-HPCS) bead on osteomyelitis management in a rat model

3.1 Infection signs

The infection signs score of infected tibia were not significantly different between pre-MRSA inoculation, pre-treatment and post-treatment during experiment in every group. Infected tibias were slightly swollen and pain (score 1-2) in the last three days after MRSA inoculation and returned to normal (score 0) after two week. Although the clinical sign was not present as osteomyelitis condition, the radiographic results revealed radiolucent area around the K-wire that indicated bone destruction.

3.2 White blood cell counts

The total white blood cell count was not significantly different between pre-inoculation and treatment period in every group. The results of total white blood cell count were showed in the table 5.

Table 5 Total white blood cell count ($\times 10^3/\mu l$) in pre-inoculation and treatment period (6 weeks).

Time	White blood cell count ($\times 10^3/\mu l$)			
	Control	GI-PMMA	G-NCS	G-HPCS
Pre-inoculation	6.63±2.23	7.06±2.50	7.06±1.91	7.12±1.10
Week 0	5.83±2.56	6.48±1.92	7.54±2.39	6.57±2.72
Week 1	6.65±2.43	8.02±2.51	8.48±3.09	7.88±2.05
Week 2	6.98±1.08	6.25±1.26	7.21±2.38	7.93±2.36
Week 3	6.69±2.10	8.32±1.93	7.90±3.29	6.46±1.66
Week 4	7.58±1.43	7.09±1.38	7.10±1.46	6.77±3.35
Week 5	7.45±1.26	7.38±1.41	6.46±1.75	7.22±2.61
Week 6	5.25±2.18	4.93±1.48	5.10±1.43	6.82±3.81

Pre-inoculation = Before inoculate MRSA, Week 0 = Treatment day, Week 1 = 7 days after treatment, Week 2 = 14 days after treatment, Week 3 = 21 days after treatment, Week 4 = 28 days after treatment, Week 5 = 35 days after treatment and Week 6 = 42 days after treatment

3.3 Radiographic examination

Infected tibias were evaluated by radiographic picture after treatment. The osteomyelitis of tibia was scored as following; do not show periosteal elevation (PE), architectural deformation (AD), widening of the bone shaft (WBS), new bone formation (NMF) and soft tissue deformation (STD). However the radiographic pictures showed percentage of radiolucent area (PRA) in different levels between the groups. The sample

radiographic pictures of control, GI-PMMA, G-NCS and G-HPCS groups were showed in the Figure 18. The radiographic scoring result was shown in the Figure 19.

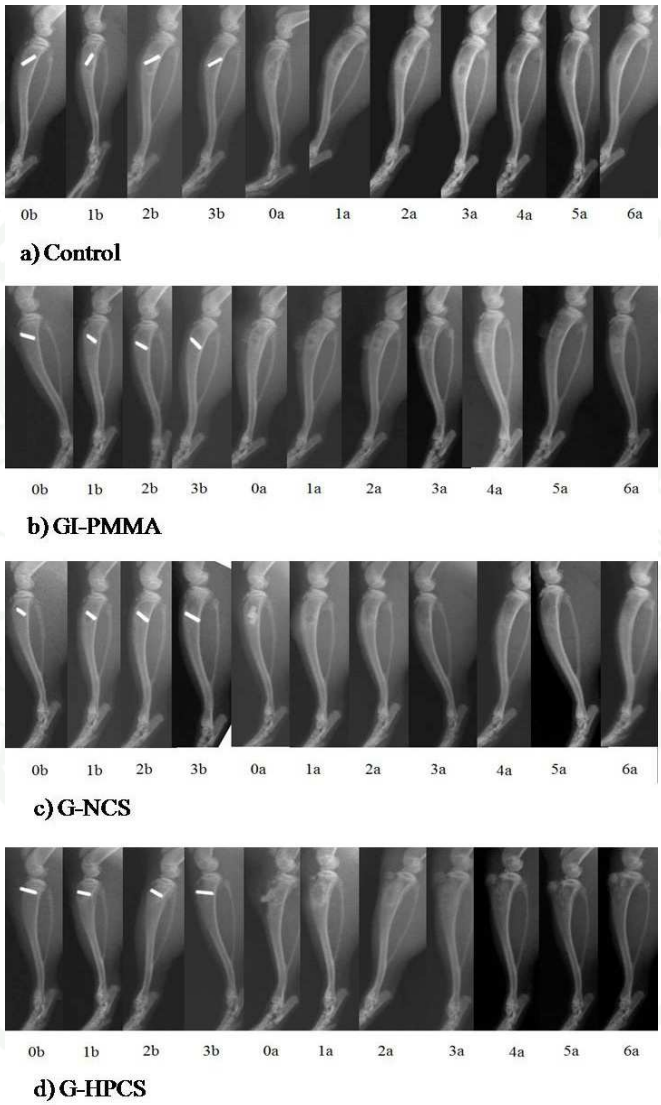

Figure 18 Radiographic pictures of tibia present in both osteomyelitis induction period and treatment period in control, GI-PMMA, G-NCS and G-HPCS group. 0b = MRSA inoculation day, 1b = 1 week after MRSA inoculation, 2b = 2 weeks after MRSA inoculation, 3b = 3 weeks after MRSA. inoculation, 0a = treatment day, 1a = 1 week after treatment, 2a = 2 weeks after treatment, 3a = 3 weeks after treatment, 4a = 4 weeks after treatment, 5a = 5 weeks after treatment, 6a = 6 weeks after treatment.

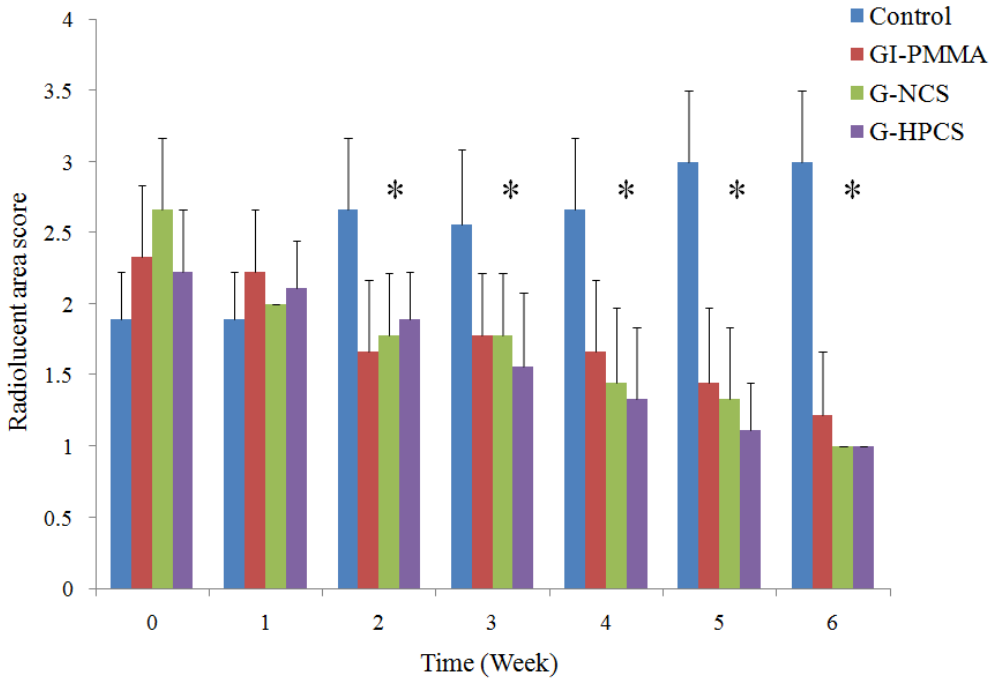

Figure 19 The radiolucent score results of control, GI-PMMA, G-NCS and G-HPCS group. * = significantly difference of radiolucent score between control group and GI-PMMA, G-NCS and G-HPCS groups.

3.4 Bone culture

After 6 weeks of treatment, bacteria colony forming unit (CFU) per gram of tissue was examined. The result was not different among groups. Average of log10 CFU/g was show in table 6. The average of bacterial growth was not different between control, GI-PMMA, G-NCS and G-HPCS.

Table 6 Bacterial growth (mean±SD of log10 CFU/g) from the infected tibias after sixth weeks of treatment.

Group	Control	GI-PMMA	G-NCS	G-HPCS
mean±SD of log10 CFU/g	3.64±0.38	3.59±0.63	3.24±0.37	3.43±0.66

3.5 Histopathological examination

All histopathological slices of control group, GI-PMMA, G-NCS and G-HPCS showed typical sign of bone infection such as abscess in bone marrow, bone sequestrum, destruction of the bone cortex and periosteal elevation. In control group, the infected tibias presented multiple fibrogranulomatous abscesses, sequestrum and destruction of corticalis (Figure 20A, 21A, 22A and 23A). In GI-PMMA group, the infected tibias showed multiple fibrogranulomatous abscesses with bone surrounding the GI-PMMA implantation site and cortical bone destruction (Figure 20B, 21B, 22B and 23B). In G-NCS and G-HPCS groups, the infected tibias appeared multiple fibrogranulomatous abscesses and new bone formation at the bone cortex without bone destruction (Figure 20C, 20D, 21C, 21D, 22C, 22D, 23C and 23D). Histopathological score of control was significantly difference from GI-PMMA, G-NCS and G-HPCS groups. The median histopathological score in control, GI-PMMA, G-NCS and G-HPCS groups were 5, 4, 3 and 3 respectively.

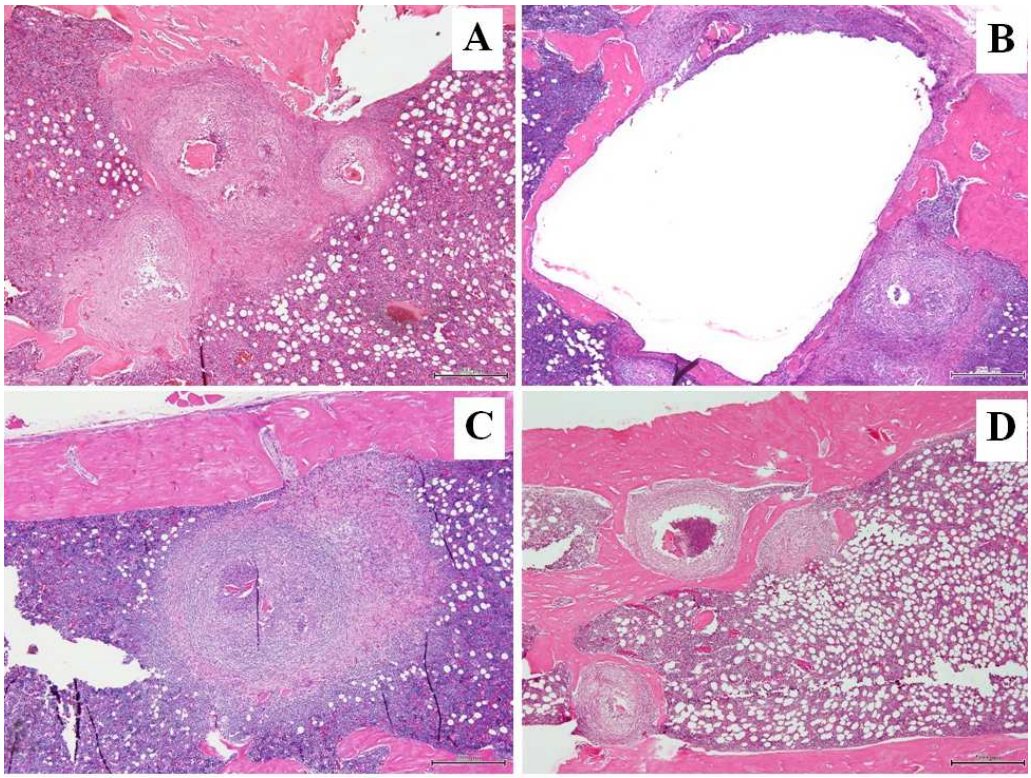

Figure 20 Bone marrow picture of control (A), GI-PMMA (B), G-NCS (C) and G-HPCS (D) H&E staining at ×400. The fibrogranulomatous abscesses and suquestrum were found in bone marrow in every group. Large space of GI-PMMA implantation site was presented in picture B.

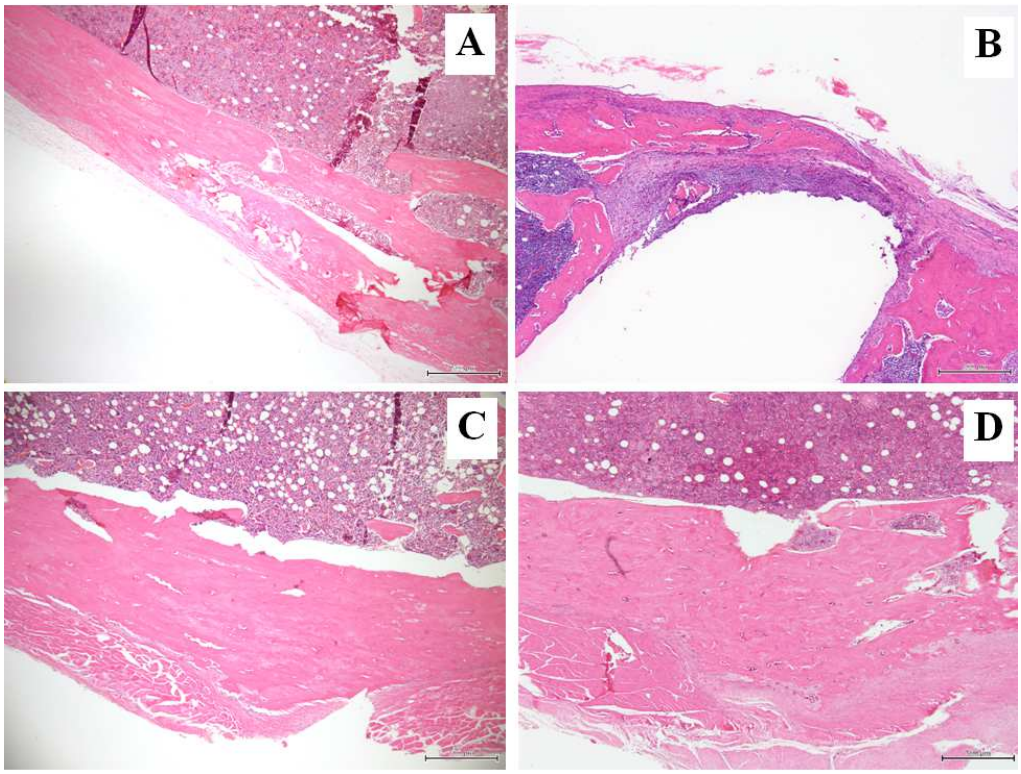

Figure 21 Bone cortex picture of control (A), GI-PMMA (B), G-NCS (C) and G-HPCS (D) H&E staining at ×400. In both control and GI-PMMA groups showed an incomplete bone cortex, while in G-NCS and G-HPCS groups was found new bone formation at the implantation sites.

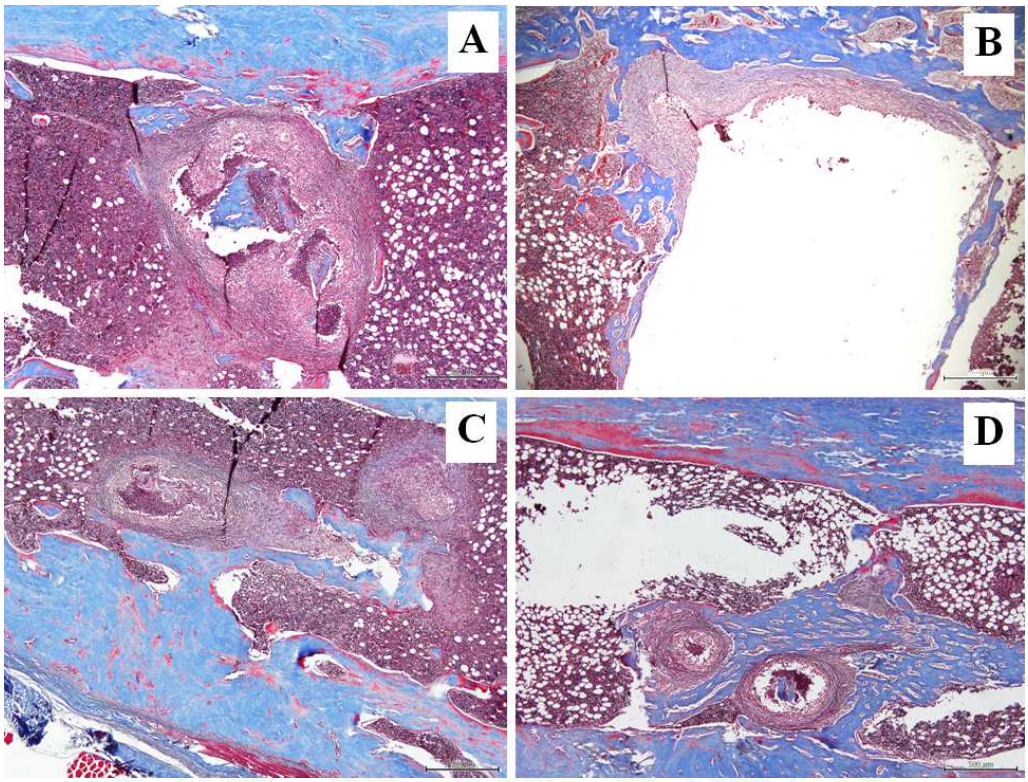

Figure 22 Bone marrow picture of control (A), GI-PMMA (B), G-NCS (C) and G-HPCS (D) Masson's trichorme staining at ×400. Characteristic of bone invaded into the bone marrow and fibrogranulomatous abscesses in the bone marrow. Large space of GI-PMMA implantation site was surrounding with fibrous tissue and bone.

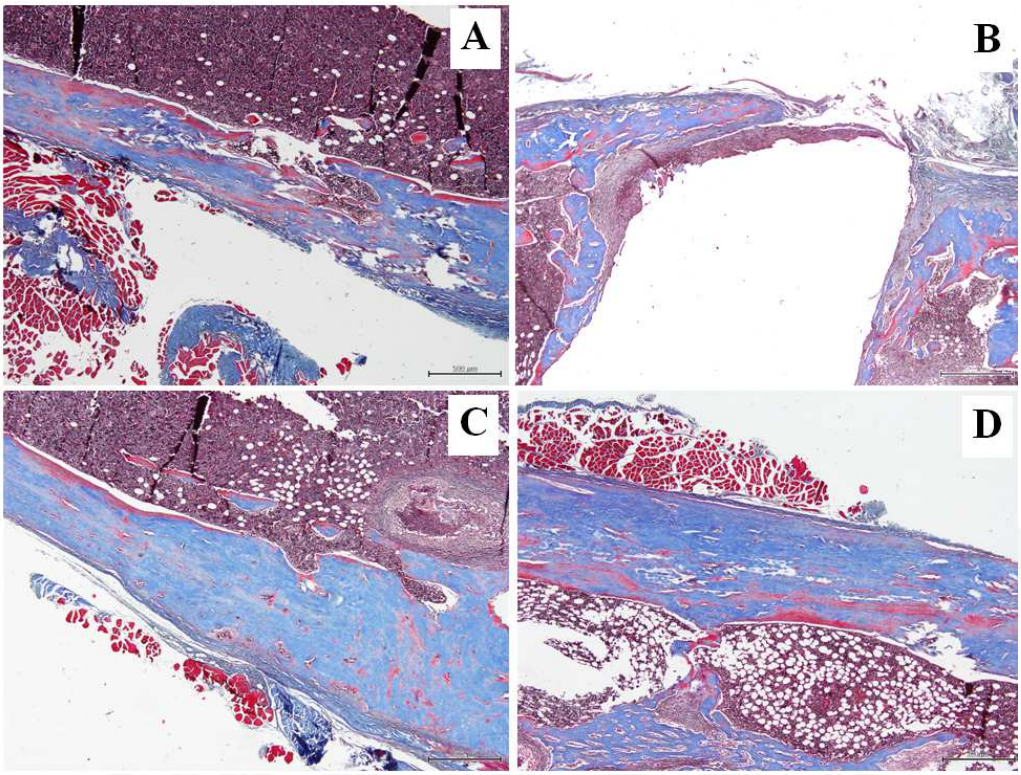

Figure 23 Bone cortex picture of control (A), GI-PMMA (B), G-NCS (C) and G-HPCS (D) Masson's trichorme staining at ×400. In both control and GI-PMMA groups showed incomplete bone cortex, while in G-NCS and G-HPCS groups showed new bone formation at the implantation sites.

DICUSSION

1. Effect of porosity of calcium sulfate beads on ceftazidime elution and *in vitro* Osteogenic properties

The application of the salt leaching technique in the present study enhanced the porosity of the calcium sulfate beads as well as positively increasing the ceftazidime elution in the *in vitro* study. Interestingly, the duration of ceftazidime released from the calcium sulfate beads was shortened as the porosity of the beads increased. The total amounts of ceftazidime released from the calcium sulfate beads with different porosity were not significantly different; however, the total amounts of eluted ceftazidime per gram of calcium sulfate bead were significantly augmented in association with an increment in the porosity of the calcium sulfate beads. Thus, the present study showed that the enhancement of calcium sulfate porosity by the salt leaching technique could enhance the amounts of ceftazidime released from the calcium sulfate beads.

The physical characteristics of the calcium sulfate beads in each group were different in total porosity, mechanical properties, water uptake capacity and mass loss. The total porosity was $19.40 \pm 3.87\%$ in the control group and increased to $48.08 \pm 3.98\%$ in the 1:1 group. The mechanical properties of maximum compressive load and maximum compressive strength were highest in the control group and rapidly decreased in the other groups and were lowest in the 1:1 group. This result was related to the calcium sulfate crystal arrangement. In the control group, the calcium sulfate crystals were approximately 10 times smaller than in the groups that underwent the salt leaching process. For this reason, the highest maximum compressive load and maximum compressive strength were found in the control group compared to the other groups. Variation in the salt leaching process led to an increase in the average crystal size; however, the average diameter of the small and large pores was not significantly different among the 4:1, 2:1 and 1:1 groups. The water uptake of the calcium sulfate beads in the study was directly related to total porosity levels. This result showed that water could fill

up the space in the calcium sulfate beads to different amounts depending on the total porosity. From the resorbable property of the calcium sulfate beads, the percentage of mass loss was studied to predict the amount of calcium sulfate remaining after a period. The mass loss of the calcium sulfate beads in each group after bathing the beads in PBS for 10 days. In the control group, mass loss percentage was the lowest when compared with the other groups. The percentage of mass loss of the calcium sulfate beads in the 4:1 group was also lower than in the 2:1 and 1:1 groups. These results indicated that the permeability levels of the calcium sulfate beads in each group were different and that the calcium sulfate beads can be dissolved in PBS.

The increased total porosity of the calcium sulfate beads had various effects on the antibiotic elution characteristic in this study. The duration of ceftazidime release from the calcium sulfate beads in each group was different. Ceftazidime in the control, 4:1, 2:1 and 1:1 groups could be detected by a microbiological assay for 6, 5, 5 and 4 days, respectively. In addition, the amounts of ceftazidime released from the calcium sulfate beads in the first day were significantly ($P < 0.0001$) higher than on the following days in all groups. The large amount of ceftazidime released in the first 24 hours may have been partly due to the releasing from the surface of the calcium sulfate beads. The concentrations of released ceftazidime in the following days from the calcium sulfate beads in every group were higher than the minimal inhibitory concentration (MIC) of *E. coli*, *Staphylococcus* spp. and *Pseudomonas aeruginosa* (Albarellos *et al*., 2008). This result revealed that the concentration of ceftazidime released from the calcium sulfate beads in every group was effective to treat the microorganisms mentioned above that caused osteomyelitis (Lazzarini *et al*., 2005).

This elution characteristic was related to the different structures of the calcium sulfate beads in each group. In the control group, the mean crystal diameter and pore size were smallest compared with the other groups. As shown in a cross sectional view, the control group had the smallest pore size and the crystal diameter, thus increasing the space for ceftazidime. Different results were found in the 4:1, 2:1 and 1:1 groups, which had big mean crystal sizes and large pores. The different porosities and pore sizes of the

calcium sulfate beads in each group had an effect on the permeability of the solution. The lowest porosity in the control calcium sulfate beads may have resulted in a longer drug elution from these beads compared to the other groups. These results suggested that the porosity levels of calcium sulfate beads have an effect on the concentration and duration of ceftazidime released from the beads through an increase in the permeability of dissolution.

Although the total amounts of ceftazidime released from the calcium sulfate beads in each group were not significantly different, the total amount of released ceftazidime in milligrams per gram weight of calcium sulfate beads was highest in the 1:1 group ($P < 0.01$). In addition, a correlation coefficient (R = 0.8152) between the amount of released ceftazidime in milligrams per gram weight of calcium sulfate beads and the total porosity was shown among the control, 4:1, 2:1 and 1:1 groups. This result showed that the porosity had an effect on the total ceftazidime released from the calcium sulfate beads when compared on an equal calcium sulfate bead weight basis and the increased porosity of the calcium sulfate beads provided more antibiotics per amount of calcium sulfate.

In the present study, only the 1:1 group had a significantly higher ratio of total amount of ceftazidime per weight of calcium sulfate beads than the control group. The improved drug delivery of the 1:1 calcium sulfate beads had a clinical implication and future prospects; therefore, the osteogenic activity was conducted on the material using human osteoblasts. The highest porous calcium sulfate beads (the 1:1 group) in this experiment had excellent compatibility and enhanced h-OBs proliferation better than the control group on both the first and the seventh days after co-incubation. The higher porosity of the calcium sulfate beads in the 1:1 group is suitable for osteoblast proliferation, since the high porosity level and the large pore size facilitated the transport of oxygen and nutrients (Takahashi *et al.*, 2004). For this reason, the high porosity calcium sulfate beads were more positive to osteoblast proliferation when compared with the control group.

Multi-level porosities of the calcium sulfate beads in the present study were created by the salt leaching process similar to those used in polymer fabrication (Reignier *et al*., 2006). The salt leaching technique is one of the particulate leaching methods. The other porogens used for generating the pores including sucrose, xylitol and erythritol (McLaren *et al*., 2007). The salt leaching method provides a simple and effective method to fabricate the material porosity by varying amounts of particulate number and size. With this technique, the percentage of porosity could increase up to 90% and pore sizes could vary between 100 and 700 µm (Hou *et al*., 2003; Reignier *et al*., 2006). Frame (1975) determined that cetrimide, a quaternary ammonium compound, can also be used as a porogen particle for calcium sulfate beads, as the cetrimide acts as a foaming agent with properties similar to other cationic surface active agents and the porosity of the calcium sulfate beads made from cetrimide depended on the concentration of cetrimide and the pressure during calcium sulfate setting. In the present study, the maximum ratio of calcium sulfate hemihydrates and sodium chloride was 1:1 w/w with a total porosity of 48.08 ± 3.98%; however, a ratio of sodium chloride higher than 50% prevented the formation of the calcium sulfate beads. The total porosity in this study could not be directly determined by the ratio of sodium chloride salt because the native calcium sulfate also was porous (19.40 ± 3.87%). Furthermore, it is possible that some sodium chloride crystals may have been dissolved during the mixing process, thus reducing the number of soluble particles.

2. Comparison of polymethylmethacrylate (PMMA) bead, native calcium sulfate (NCS) bead, and high porous calcium sulfate (HPCS) bead as gentamicin carriers and osteoblast attachment.

Physical properties of commercial PMMA beads (GI-PMMA and G-PMMA), G-NCS and G-HPCS beads were distinct in weight, total porosity, water uptake capacity, and mass loss. PMMA beads (GI-PMMA=119.38±7.45 mg and G-PMMA=117.93±8.36 mg) were lighter than G-NCS beads (163.08±5.73 mg). However, the G-HPCS bead was the lightest one (84.92±6.38 mg) since the salt leach increased its porosity up to 42.32±4.57%. According to water uptake capacity depended on total porosity, GI-PMMA

and G-PMMA beads had less such capacity since their total porosity was lower than that of calcium sulfate beads. For mass loss property, the G-HPCS bead had the highest percentage (9.19±1.52%) of mass loss after 10 days of the experiment. Since PMMA bead was a non-dissolvable material, the mass loss in this study was from getamicin release. A number of studies reported that polymers coated on the material were used for facilitating the release of growth factor (Choi *et al*., 2011; Lee *et al*., 2010). In some studies, antibiotic release was controlled by coated material with thin polymer layer containing antibiotic (Osaki *et al*., 2012; Vasilev *et al*., 2011). The mass loss of G-HPCS bead might be reduced by coating the material with polymer; it might slow down antibiotic release from G-HPCS surface.

Human osteoblasts (h-OBs) could survive in HPCS, NCS, and PMMA beads when observed with scanning electron microscope. The present study demonstrated that NCS and PMMA beads were non-toxic materials to h-OBs. This was in agreement with the previous study conducted in mouse's osteoblast (MC3T3-E1) (Lazary *et al*., 2007). . That study revealed that MC3T3-E1 could proliferate two-fold in gypsum when compared with PMMA in the first 24 hours. Furthermore, they found the alkaline phosphatase activity and SMAD3 expression in the gypsum group were higher than in PMMA group. However, our study showed that the new type of calcium sulfate bead, HPCS, had a high potential for use as an osteoconductive material similar to NCS bead, while PMMA bead did not have this property.

The microbiological assay using *Bacillus subtilis* (ATCC 6633) was an agar diffusion method for estimating the released antibiotic. The amount of gentamicin released from the bead each day was calculated according to this assay. The elution kinetics of gentamicin from GI-PMMA, G-PMMA, G-NCS and G-HPCS beads was significantly different. The total amount of gentamicin in G-PMMA, G-NCS and G-HPCS beads could be quantified by area under the curve, while gentamicin amount per bead in GI-PMMA was calculated by percent concentration of gentamicin per weight of the bead. This study found that only small amount of gentamicin (16.32±7.22% of total gentamicin) could be eluted from GI-PMMA during 10-day experiment. This

corresponded with the previous report that only 5-8% of antibiotic in PMMA was released from the exposed surface during the first week (Wahlig *et al.*, 1980). In contrast, most of gentamicin (99-100%) could be eluted from G-PMMA, G-NCS and G-HPCS beads. These results were likely due to the differences in gentamicin coating method. The release of gentamicin could be separated into two phases: initial and sustain phases. This phenomenon was reported in many previous studies (Hendriks *et al*., 2004; Udomkusonsri *et al*., 2010; Belt *et al*., 2000; Wichelhaus *et al*., 2001). Likewise, the present study found that such phenomenon took place with GI-PMMA, G-PMMA, G-NCS, and G-HPCS beads. Most of gentamicin was eluted from the beads within the first day, known as an initial phase and followed by a sustain phase until the tenth day in GI-PMMA, G-NCS, and G-HPCS beads. However, the previous study found that 80% of gentamicin was released from G-NCS bead within the first day (Wichelhaus *et al.*,2001). This might be due to the amount of solution used for dissolving gentamicin from the beads. The previous experiment used 5 ml PBS, while 1 ml of PBS was used in the present study. One milliliter of PBS might be saturated with gentamicin in the first day in our experiment. For G-PMMA bead, the gentamicin could be detected in a short period since PMMA had fewer pores on its surface and did not have interconnecting pores. Thus, PMMA could uptake antibiotic only in a low level when it was already in hardening form, owing to the porosity of the bead contributed to the permeability to the bead matrix. The higher porosity was found in G-HPCS bead than in G-NCS bead, resulting in the higher percentage of gentamicin released from G-HPCS bead in the initial phase than that of G-NCS bead.

Gentamicin could coat only on the surface and superficial layer of the matrix . The elution characteristic of G-PMMA bead was different from GI-PMMA bead. GI-PMMA could release gentamicin until the end of the experiment, because gentamicin was added to PMMA prior to be hardened and was incorporated into the matrix of the materials. Antibiotic selection was limited for producing PMMA antibiotic beads since it needed a high temperature for the polymerization (Nandi *et al*., 2009). In this study, it was found that the antibiotic was inappropriate to be added to PMMA after hardening process. In addition, gentamicin concentration eluted from GI-PMMA and G-PMMA

beads were lower than that of G-NCS and G-HPCS beads in the total amount. Our results suggested that PMMA bead had lower ability as a local drug-release agent compared to calcium sulfate bead.

The G-HPCS bead was a new type of calcium sulfate bead used in the present study. It had high porosity, high antibiotic uptake and release. Furthermore, HPCS bead was non-toxic to h-OBs and provided a positive effect on h-OBs attachment. G-HPCS and G-NCS beads could provide high concentration of gentamicin during the experiment. Although G-NCS bead could provide higher amount of gentamicin than G-HPCS bead after the second day through the end of study, the concentration of gentamicin released from G-HPCS was not lower than from GI-PMMA until the end of the study. These concentrations were above minimal inhibition concentration (MIC) for pathogenic bacteria, *Staphylococcus aureus*, which normally caused osteomyelitis exhibiting an MIC_{90} value (antibiotic concentration which inhibited the growth of susceptible strain *S. aureus* by 90%) of 1 μg/ml for gentamicin in susceptible strains (Fluit *et al*., 2000). From these reasons, the G-HPCS bead could be as applied as a local antibiotic delivery vehicle. Comparing the elution characteristics between G-NCS and G-HPCS beads, it was found that the concentration of gentamicin released from G-HPCS bead in the first day was higher than from G-NCS bead, then rapidly decreased on the following day. This result was a consequence of the difference in porosity level and water uptake capacity of the bead in each group, leading to a faster dissolution of gentamicin from G-HPCS than from G-NCS. This result was similar to a previous study, which showed the difference of gentamicin and vancomycin releases from nanocrystalline hydroxyapatite and calcium sulfate beads (Rauschmann *et al.*, 2005). The nanocrystalline hydroxyapatite in combination with calcium sulfate exhibited a higher porosity and water uptake capacity than pure calcium sulfate. These properties led to a higher antibiotic uptake and faster release of gentamicin and vancomycin within the first day by the composite material (Rauschmann *et al*., 2005). The results of our study also correlated with a previous study regarding the different phases of surface roughness, porosity, and wettability of gentamicin-loaded bone cements (Belt *et al*., 2000). They concluded that the releasing kinetics of gentamicin from bone cements was controlled by a combination of surface

roughness and porosity. Interestingly, many previous studies showed the disadvantage of calcium sulfate as it might cause a transient cytotoxic effect, leading to inflammatory reactions (Coetzee *et al*., 1980; Lee *et al*., 2002; Robinson *et al*., 1999). It resulted in more acidic microenvironment followed by a local inflammation at the site of implantation in human bone (Coetzee *et al*., 1980). From this reason, the G-HPCS bead had an advantage over the G-NCS bead since the amount of calcium sulfate per bead of G-HPCS was significantly lower than G-NCS bead. An application of G-HPCS bead could reduce the side effects of calcium sulfate when implanted in the tissue.

The present study introduced a practical technique to apply a new type of calcium sulfate bead as local antibiotic delivery vehicle. The G-HPCS bead eluted higher concentration of gentamicin than GI-PMMA and G-PMMA beads. Moreover, G-HPCS bead was cheaper than PMMA bead and was easier to prepare with gentamicin sulfate in a clinical setting. Furthermore, gentamicin sulfate could be added to calcium sulfate beads after the hardening procedure. The advantages of dipping antibiotic in post-hardening calcium sulfate bead included the facilitation of individualized antibiotic therapy and the prevention of antibiotic degradation owing to the sterilization process or thermal instability (Dacquet *et al*., 1992).

3. Efficiency of gentamicin impregnated polymethlymetacrylate (GI-PMMA) bead, gentamicin coated native calcium sulfate (G-NCS) bead and gentamicin coated high porous calcium sulfate (G-HPCS) bead on osteomyelitis management in a rat model

Osteomyelitis is a serious condition in both human and animal medicine. The management of ostemyelitis is quite difficult because of the poor vascularization at the infected area from the necrosis of the surrounding soft tissue. Localized antibiotic administration is used for provide high concentration of antibiotic in the infected site without systemic side effect. Commercial gentamicin impregnated PMMA is widely used as commercial local antibiotic provider. The calcium sulfate bead is an alternative system for used as local antibiotic provider. The high porous calcium sulfate (HPCS) bead was developed in this study to reducing the side effect of the calcium sulfate and to use as a

local antibiotic provider as same as calcium sulfate bead. A study showed the difference of the porosity level of calcium sulfate bead that has an effect on the antibiotic releasing in an *in vitro* study and high porous calcium sulfate bead could provide antibiotic in the highest concentration when compared in weight of calcium sulfate (Thitiyanaporn *et al*., 2012). The ostemyelitis management result of this study was similar in group GI-PMMA, G-NCS and G-HPCS. However the GI-PMMA bead is a non-absorbable material, it has to be removed after a period of time, while G-NCS and G-HPCS are absorbable material. After GI-PMMA was removed, the wide space of the implanted bone cortex still remained. This space may result of the bone fracture from instability of the effected bone.

There are numerous reports of rat osteomyelitis model developed for studying in pathogenesis, diagnosis and osteomyelitis management. In our study, the rat osteomyelitis was modified from the experiment of Orchan *et al.* (2009) and Monzón *et al*. (2001). Orchan *et al.* (2009) developed the rat osteomyelitis model in rat tibia by injection 200 µl of methicillin resistance *S.aureus* (MRSA) containing 1.0×10^7 CFU/ml and implant Kirchner wire (5.0× 1.0 mm) to the bone marrow cavity. The bone hole was sealed with dental gypsum and waiting for 3 months for develop the chronic osteomyelitis (Orhan *et al*., 2009). For the experiment of Monzónv et al. (2001), developed the osteomyelitis model by implanting the Kirchner wire coated with biofilm of the *S.aureus* to the bone marrow and 42 days of chronic osteomyelitis development was allowed (Monzon *et al*., 2001). Our study used 500 µl of MRSA 4.0×10^7 CFU/ml and implanted a Kirchner wire (5.0× 1.0 mm) coated with biofilm of MRSA. The osteomyelitis was allowed to develop for 21 days. The osteomyelitis was developed in only bone marrow cavity and did not effect to the other parts of bone. However, in a study of Fukushima 2005, they injected the *S.aureus* strain BB in the wistar rat tibia in many concentrations consisted of control = 0 CFU/5 µl, G1 = 6×10 CFU/5 µl, G2 = 6×10^2 CFU/5 µl, G3 = 6×10^3 CFU/5 µl, G4 = 6×10^4 CFU/5 µl and G5 = 6×10^5 CFU/5 µl and closed the tibial hole with bone wax. The osteomyelitis was allowed for develop within 1 week and the osteomyelitis was assessed in radiographic and histophatological examination. The recommend dose was G3 = 6×10^3 CFU/5 µl sufficient for develop osteomyelitis condition in rat tibia (Fukushima *et al*., 2005). The last decade studies

showed that the necrotic agent was not necessary for develop ostemyelitis condition in rat model (Fukushima *et al*., 2005; Gisby *et al*., 1994; Monzon *et al*., 2001; Nelson *et al*., 1990; Orhan *et al*., 2009) as the previous studies (Mendel *et al*., 1999; Norden *et al*., 1970; Rissing *et al*., 1985). The osteomyelitis model in rat was not created only in tibia but also in femur (Chen *et al*., 2005), mandible (Chistov *et al*., 1989; Shvyrkov *et al*., 1981) and hematogenous route (Hienz *et al*., 1995; Kadyrov *et al*., 1966).

The rat ostemyelitis model in current study did not affect the weight, infection signs score and white blood cell count. This result was due to the infection that limited only in the marrow cavity. The deterioration of bone structure may happen if the ostemyelitis condition was allowed to continue to 42 days (Brin *et al*., 2008; Monzon *et al*., 2001) or 3 months (Orhan *et al*., 2009) as the previous experiments. However, after 3 weeks of osteomyelitis, induction in this study showed osteomyelitis signs in the radiographic examination. The radiographic study showed the radiolucent area in the bone marrow cavity surrounding the inoculation site. After treatment, the control group was continuously wide; while radiolucent area in GI-PMMA, G-NCS and G-HPCS were significantly decrease. This result suggested that the GI-PMMA, G-NCS and G-HPCS could be used for managing osteomyelitis. For histopathological study in H&E and Masson's trichrome staining, the sequestrums, fibrogranulomatous abscess and bone cortex deterioration was observed in the control group, while G-NCS and G-HPCS were found the thickening of bone cortex at the implantation site. This result suggests that the calcium sulfate beads could facilitate the new bone regeneration. Although the results of GI-PMMA on treatment of osteomyelitis in this study were satisfied, the wide space of the bone cortex and bone marrow was found in this study.

The study of local antibiotic delivery for treatment ostemyelitis was not limited only in bone cement and calcium sulfate but also the types of antibiotic was not limited only in gentamicin. Many recent studies showed various types of material for using as the local antibiotic carrier such as hydroxyapatite cement/vancomycin (Joosten *et al*., 2005), porous calcium phosphate/cefuroxime (Nandi *et al*., 2009), poly (D,L-lactide) and calcium phosphate/ciprofloxacin (Alvarez *et al*., 2008). Many studies of calcium sulfate

bead had been developed for increasing efficiency for the treatment of ostemyelitis in prolong the concentration of antibiotic at the local area such as a study in 2009, they developed liposomal gentamicin-impregnated calcium sulfate for preventing biofilm bacterial infection that had effective than gentamicin-impregnated calcium sulfate bead (Hui *et al*., 2009). In addition to combine liposome with calcium sulfate, the calcium sulfate could be coated by polysaccharide such as chitosan for reducing rate of the degradation and prolonged the antibiotic releasing in the local tissue (Noel *et al*., 2008).

CONCLUSION AND RECOMMENDATION

The porosity of calcium sulfate bead could be increased by salt leaching technique. The highest ratio between salt and calcium sulfate hemihydrate was 1:1 w/w. This ration could increase the total porosity of calcium sulfate up to 50% from 30 % in native calcium sulfate (NCS) bead. The highest porosity of calcium sulfate in this study was called “high porous calcium sulfate (HPCS) bead”. From this study, the different levels of porosity could alternate the characteristic of antibiotic releasing. These experiments of two types of antibiotics were studied including of ceftazidime and gentamicin in pattern of antibiotic release in *in vitro* studies. The compatibility of calcium sulfate and polymethylmethacrylate (PMMA) with human osteoblast (h-OBs) was studied. The HPCS showed positive on osteoblast proliferation when compared with NCS and PMMA. In an experiment of GI-PMMA, G-NCS and G-HPCS beads on efficiency of osteomyelitis management in a rat model, showed the GI-PMMA, G-NCS and G-HPCS beads were the same result but different from the control group. However, GI-PMMA bead had to be removed after 6 weeks and the bone hole was present in the tibia cortex, whereas G-NCS and G-HPCS beads group the bone cortex was healed normally.

For the experiment of different porosity level on ceftazidime releasing, showed the salt leaching technique could increased the total porosity of the calcium sulfate beads. The increased porosity of the calcium sulfate beads led to an enhanced ceftazidime elution; however, this reduced the duration of drug releasing. The porosity of the calcium sulfate beads had an effect on drug releasing by increasing the surface area of the calcium sulfate beads and promoting the dissolution of ceftazidime. Although the duration of ceftazidime released from the calcium sulfate beads in the control group was longer than in the 1:1 group, the accumulative amount of ceftazidime was not different. In addition, the high porosity of the calcium sulfate beads enhanced osteoblast proliferation compared to the control calcium sulfate beads. In summary, the high porosity calcium sulfate beads effectively improved the drug elution and could be used as a drug delivery vehicle. On

the other hand, the enhanced osteogenesis of the high porosity calcium sulfate beads warrants their used as a bone substitute material.

In the study of gentamicin released from GI-PMMA, G-PMMA, G-NCS and G-HPCS, the study introduced a practical technique to apply a new type of calcium sulfate bead as local antibiotic delivery vehicle. The G-HPCS bead eluted gentamicin at a higher level than GI-PMMA and G-PMMA beads. G-HPCS bead is cheaper than PMMA bead and is easier to prepare with gentamicin sulfate in a clinical setting. Furthermore, the gentamicin sulfate could be added to calcium sulfate beads after hardening. The advantages of dipping antibiotic in post hardening calcium sulfate bead including facilitation of individualized antibiotic therapy and prevention of antibiotic degradation owing to the sterilization process or thermal instability reduces the activity of antibiotic. In addition, G-HPCS beads in this study not only improved local antibiotic delivery but also had a positive effect on osteoblast proliferation that essential on new bone regeneration in osteomyelitis condition.

Rat osteomyelitis condition was treated with three different gentamicin beads**.** From the result showed that the G-HPCS had efficiency to manage the osteomyelitis the same as commercial gentamicin impregnated PMMA (GI-PMMA) and G-NCS. This reason suggested that the HPCS was a new type of calcium sulfate bead and could be used as antibiotic carrier. Although the clinical signs and white blood cell count in this experiment were not significantly different between the control and treatment groups, the radiographic and histopathologic results of GI-PMMA, G-NCS and G-HPCS were improved than control group. In the result of GI-PMMA bead, it provided result of osteomyelitis management as same as G-HPCS and G-NCS. However, the GI-PMMA bead had to be removed at the end of treatment, the PMMA was not absorbable material and the surface of the PMMA could be coated with the host protein and facilitated bacterial colonization and made large dead space in the bone cortex and soft tissue, while in G-NCS and G-HPCS were resorbable beads. From this reason, the GI-PMMA might cause the bone fracture after PMMA removal. G-HPCS could be reduced the side effect

of G-NCS by decreasing amount of calcium sulfate dihydrate that had evidence to increase acidic condition in the implant area and created local inflammation.

Although the HPCS is a new type of calcium sulfate bead that can be used as an antibiotic carrier and used for osteomyelitis management, the HPCS can be improved in the future experiment by coat with biodegradable material or integrate with other materials for increasing the duration of pharmacological agents release and decreasing degradable time. Recently, other pharmacological agents were not studied with HPCS bead. Coating of bone morphogenetic proteins (BMPs), transforming growth factor-β (TGF-β), platelet derived growth factors (PDGF) and other new bone inducing agents on HPCS bead are interesting to be studied for facilitating bone healing.

LITERATURE CITED

Abdul-Karim, F.W., M.G. McGinnis, M. Kraay, S.N. Emancipator and V. Goldberg. 1998. Frozen Section Biopsy Assessment for the Presence of Polymorphonuclear Leukocytes in Patients Undergoing Revision of Arthroplasties. **Mod Pathol**. 11 (5): 427-431.

al Ruhaimi, K.A. 2001. Effect of Calcium Sulphate on the Rate of Osteogenesis in Distracted Bone. **Int J Oral Maxillofac Surg**. 30 (3): 228-233.

Albarellos, G.A., L.A. Ambros and M.F. Landoni. 2008. Pharmacokinetics of Ceftazidime after Intravenous and Intramuscular Administration to Domestic Cats. **The Veterinary Journal**. 178: 238–243.

Alvarez, H., C. Castro, L. Moujir, A. Perera, A. Delgado, I. Soriano, C. Evora and E. Sanchez. 2008. Efficacy of Ciprofloxacin Implants in Treating Experimental Osteomyelitis. **J Biomed Mater Res B Appl Biomater**. 85 (1): 93-104.

Anagnostakos, K. and J. Kelm. 2009. Enhancement of Antibiotic Elution from Acrylic Bone Cement. **J Biomed Mater Res B Appl Biomater**. 90 (1): 467-475.

Anusavice, K.J. 2003. **Phillips' Science of Dental Materials**. Saunders elsevier, St. Louis, Missouri.

Apaydin, E.S. and M. Torabinejad. 2004. The Effect of Calcium Sulfate on Hard-Tissue Healing after Periradicular Surgery. **J Endod**. 30 (1): 17-20.

Bach, M.C. and D.M. Cocchetto. 1987. Ceftazidime as Single-Agent Therapy for Gram-Negative Aerobic Bacillary Osteomyelitis. **Antimicrob Agents Chemother**. 31 (10): 1605-1608.

Bahn, S.L. 1966. Plaster: A Bone Substitute. **Oral Surg Oral Med Oral Pathol**. 21 (5): 672-681.

Baro, M., E. Sanchez, A. Delgado, A. Perera and C. Evora. 2002. In Vitro-in Vivo Characterization of Gentamicin Bone Implants. **J Control Release**. 83 (3): 353-364.

Bennett, J.V., J.L. Brodie, E.J. Benner and W.M. Kirby. 1966. Simplified, Accurate Method for Antibiotic Assay of Clinical Specimens. **Appl Microbiol**. 14 (2): 170-177.

Benoit, M.A., B. Mousset, C. Delloye, R. Bouillet and J. Gillard. 1997. Antibiotic-Loaded Plaster of Paris Implants Coated with Poly Lactide-Co-Glycolide as a Controlled Release Delivery System for the Treatment of Bone Infections. **Int Orthop**. 21 (6): 403-408.

Beuerlein, M.J. and M.D. McKee. 2010. Calcium Sulfates: What Is the Evidence? **J Orthop Trauma**. 24 (Suppl 1): S46-51.

Bignon, A., J. Chouteau, J. Chevalier, G. Fantozzi, J.P. Carret, P. Chavassieux, G. Boivin, M. Melin and D. Hartmann. 2003. Effect of Micro- and Macroporosity of Bone Substitutes on Their Mechanical Properties and Cellular Response. **J Mater Sci Mater Med**. 14 (12): 1089-1097.

Brady, R.A., L.G. Leid, J.W. Costerton and M.E. Shirtliff. 2006. Osteomyelitis: Clinical Review and Mechanisms of Infection Persistance. **Clinical microbiology newsletter**. 28 (9): 65-72.

Brin, Y.S., J. Golenser, B. Mizrahi, G. Maoz, A.J. Domb, S. Peddada, S. Tuvia, A. Nyska and M. Nyska. 2008. Treatment of Osteomyelitis in Rats by Injection of

Degradable Polymer Releasing Gentamicin. **J Control Release**. 131 (2): 121-127.

Bruckschen, B., H. Seitz, T.M. Buzug, C. Tille, B. Leukers and S. Irsen. 2005. Comparing Different Porosity Measurement Methods for Characterisation of 3D Printed Bone Replacement Scaffolds. **Biomedizinische Technik.** 50 (Suppl 1 - Part 2): 1609-1610.

Chen, X., D.T. Tsukayama, L.S. Kidder, C.A. Bourgeault, A.H. Schmidt and W.D. Lew. 2005. Characterization of a Chronic Infection in an Internally-Stabilized Segmental Defect in the Rat Femur. **J Orthop Res**. 23 (4): 816-823.

Chistov, V.B. 1989. The Effect of Low-Intensity Radiation from a Helium-Neon Laser on the Alkaline Phosphatase Activity in an Uncomplicated Mandibular Fracture and in Traumatic Osteomyelitis. **Stomatologiia**. 68 (6): 13-15.

Cho, B.C., T.G. Kim, J.D. Yang, H.Y. Chung, J.W. Park, I.C. Kwon, K.H. Roh, H.S. Chung, D.S. Lee, N.U. Park and I.S. Kim. 2005. Effect of Calcium Sulfate-Chitosan Composite: Pellet on Bone Formation in Bone Defect. **J Craniofac Surg**. 16 (2): 213-224.

Choi, S., J.K. Lee, S. Igawa, M. Suzuki, R. Mochizuki, U.I. Nishimura and N. Sasaki. 2011. Effect of Trehalose Coating on Basic Fibroblast Growth Factor Release from Tailor-Made Bone Implants. **J Vet Med Sci**. 73 (12): 1547-1552.

Cierny, G., J.T. Mader and J.J. Penninck. 2003. A Clinical Staging System for Adult Osteomyelitis. **Clin Orthop Relat Res**. 414: 7-24.

Coetzee, A.S. 1980. Regeneration of Bone in the Presence of Calcium Sulfate. **Arch Otolaryngol** 106. 7: 405-409.

Cui, X., D. Zhao, B. Zhang and Y. Gao. 2009. Osteogenesis Mechanism of Chitosan-Coated Calcium Sulfate Pellets on the Restoration of Segmental Bone Defects. **J Craniofac Surg**. 20 (5): 1445-1450.

Dacquet, V., A. Varlet, R.N. Tandogan, M.M. Tahon, L. Fournier, F. Jehl, H. Monteil and G. Bascoulergue. 1992. Antibiotic-Impregnated Plaster of Paris Beads. Trials with Teicoplanin. **Clin Orthop Relat Res**. 282: 241-249.

Damien, C.J. and J.R. Parsons. 1991. Bone Graft and Bone Graft Substitutes: A Review of Current Technology and Applications. **J Appl Biomater**. 2 (3): 187-208.

Doadrio, J.C., D. Arcos, M.V. Cabanas and M. Vallet-Regi. 2004. Calcium Sulphate-Based Cements Containing Cephalexin. **Biomaterials**. 25 (13): 2629-2635.

Elasri, M.O., J.R. Thomas, R.A. Skinner, J.S. Blevins, K.E. Beenken, C.L. Nelson and M.S. Smeltzer. 2002. Staphylococcus Aureus Collagen Adhesin Contributes to the Pathogenesis of Osteomyelitis. **Bone**. 30 (1): 275-280.

Eron, L.J., C.H. Park, D.L. Hixon, R.I. Goldenberg and D.M. Poretz. 1983. Ceftazidime in Patients with Pseudomonas Infections. **J Antimicrob Chemother**. 12 (Suppl A): 161-169.

Ficker, L., T.A. Meredith, S. Gardner and L.A. Wilson. 1990. Cefazolin Levels after Intravitreal Injection. Effects of Inflammation and Surgery. **Invest Ophthalmol Vis Sci**. 31 (3): 502-505.

Fihman, V., D. Hannouche, V. Bousson, T. Bardin, F. Liote, L. Raskine, J. Riahi, M.J. Sanson-Le Pors and B. Bercot. 2007. Improved Diagnosis Specificity in Bone and Joint Infections Using Molecular Techniques. **J Infect**. 55 (6): 510-517.

Fluit, A.C., M.E. Jones, F.J. Schmitz, J. Acar, R. Gupta and J. Verhoef. 2000. Antimicrobial Susceptibility and Frequency of Occurrence of Clinical Blood Isolates in Europe from the Sentry Antimicrobial Surveillance Program, 1997 and 1998. **Clin Infect Dis**. 30 (3): 454-460.

Frame, J.W. 1975. Porous Calcium Sulphate Dihydrate as a Biodegradable Implant in Bone. **J Dent**. 3 (4): 177-187.

Fukushima, N., K. Yokoyama, T. Sasahara, Y. Dobashi and M. Itoman. 2005. Establishment of Rat Model of Acute Staphylococcal Osteomyelitis: Relationship between Inoculation Dose and Development of Osteomyelitis. **Arch Orthop Trauma Surg**. 125 (3): 169-176.

Gao, C., S. Huo, X. Li, X. You, Y. Zhang and J. Gao. 2007. Characteristics of Calcium Sulfate/ Gelatin Composite Biomaterials for Bone Repair. **J Biomater Sci Polym Ed**. 18 (7): 799-824.

Gentry, L.O. 1997. Management of Osteomyelitis. **Int J Antimicrob Agents**. 9 (1): 37-42.

Gisby, J., A.S. Beale, J.E. Bryant and C.D. Toseland. 1994. Staphylococcal Osteomyelitis--a Comparison of Co-Amoxiclav with Clindamycin and Flucloxacillin in an Experimental Rat Model. **J Antimicrob Chemother**. 34 (5): 755-764.

Gitelis, S. and G.T. Brebach. 2002. The Treatment of Chronic Osteomyelitis with a Biodegradable Antibiotic-Impregnated Implant. **J Orthop Surg (Hong Kong)**. 10 (1): 53-60.

Gondusky, J.S., C.J. Gondusky and S.W. Helmers. 2009. Salmonella Osteomyelitis in New-Onset Diabetes Mellitus. **Orthopedics**. 32 (9): pii: orthosupersite.com/view. asp?rID=42857. doi: 10.3928/01477447-20090728-42.

Gotz, F. 2002. Staphylococcus and Biofilms. **Mol Microbiol**. 43 (6): 1367-1378.

Groeneveld, E.H., J.P. van den Bergh, P. Holzmann, C.M. ten Bruggenkate, D.B. Tuinzing and E.H. Burger. 1999. Mineralization Processes in Demineralized Bone Matrix Grafts in Human Maxillary Sinus Floor Elevations. **J Biomed Mater Res**. 48 (4): 393-402.

Habibovic, P., H. Yuan, C.M. van der Valk, G. Meijer, C.A. van Blitterswijk and K. de Groot. 2005. 3D Microenvironment as Essential Element for Osteoinduction by Biomaterials. **Biomaterials**. 26 (17): 3565-3575.

Ham, K., D. Griffon, M. Seddighi and A.L. Johnson. 2008. Clinical Application of Tobramycin-Impregnated Calcium Sulfate Beads in Six Dogs (2002-2004). **J Am Anim Hosp Assoc**. 44 (6): 320-326.

Hendriks, J.G., J.R. van Horn, H.C. van der Mei and H.J. Busscher. 2004. Backgrounds of Antibiotic-Loaded Bone Cement and Prosthesis-Related Infection. **Biomaterials**. 25 (3): 545-556.

Hienz, S.A., H. Sakamoto, J.I. Flock, A.C. Morner, F.P. Reinholt, A. Heimdahl and C.E. Nord. 1995. Development and Characterization of a New Model of Hematogenous Osteomyelitis in the Rat. **J Infect Dis**. 171 (5): 1230-1236.

Hing, K.A., S.M. Best, K.E. Tanner, W. Bonfield and P.A. Revell. 2004. Mediation of Bone Ingrowth in Porous Hydroxyapatite Bone Graft Substitutes. **J Biomed Mater Res A**. 68 (1): 187-200.

Hing, K.A., B. Annaz, S. Saeed, P.A. Revell and T. Buckland. 2005. Microporosity Enhances Bioactivity of Synthetic Bone Graft Substitutes. **J Mater Sci Mater Med**. 16 (5): 467-475.

Hou, Q., D.W. Grijpma and J. Feijen. 2003. Porous Polymeric Structures for Tissue Engineering Prepared by a Coagulation, Compression Moulding and Salt Leaching Technique. **Biomaterials**. 24 (11): 1937-1947.

Howard, C.B., M. Einhorn, R. Dagan and M. Nyska. 1995. Ultrasonic Features of Acute Osteomyelitis. **J Bone Joint Surg Br**. 77 (4): 663-664.

Hui, T., X. Yongqing, Z. Tiane, L. Gang, Y. Yonggang, J. Muyao, L. Jun and D. Jing. 2009. Treatment of Osteomyelitis by Liposomal Gentamicin-Impregnated Calcium Sulfate. **Arch Orthop Trauma Surg**. 129 (10): 1301-1308.

Hulbert, S.F., F.A. Young, R.S. Mathews, J.J. Klawitter, C.D. Talbert and F.H. Stelling. 1970. Potential of Ceramic Materials as Permanently Implantable Skeletal Prostheses. **J Biomed Mater Res**. 4 (3): 433-456.

Hutmacher, D.W., T. Schantz, I. Zein, K.W. Ng, S.H. Teoh and K.C. Tan. 2001. Mechanical Properties and Cell Cultural Response of Polycaprolactone Scaffolds Designed and Fabricated Via Fused Deposition Modeling. **J Biomed Mater Res**. 55 (2): 203-216.

Intini, G., S. Andreana, F.E. Intini, R.J. Buhite and L.A. Bobek. 2007. Calcium Sulfate and Platelet-Rich Plasma Make a Novel Osteoinductive Biomaterial for Bone Regeneration. **J Transl Med**. 5: 13.

Jin, Q.M., H. Takita, T. Kohgo, K. Atsumi, H. Itoh and Y. Kuboki. 2000. Effects of Geometry of Hydroxyapatite as a Cell Substratum in Bmp-Induced Ectopic Bone Formation. **J Biomed Mater Res**. 52 (4): 491-499.

Joe¨l, R. and M.A. Huneault. 2006. Preparation of Interconnected Poly (3-Caprolactone) Porous Scaffolds by a Combination of Polymer and Salt Particulate Leaching. **Polymer**. 47: 4703–4717.

Jones, J.T. and M. F. Berard. 1993. Physical Measurments, pp 156-177. in J. T. Jones, Berard , M.F., eds. **Ceramics Industrial Processing and Testing.** Iowa State University Press, Iowa.

Joosten, U., A. Joist, G. Gosheger, U. Liljenqvist, B. Brandt and C. von Eiff. 2005. Effectiveness of Hydroxyapatite-Vancomycin Bone Cement in the Treatment of Staphylococcus Aureus Induced Chronic Osteomyelitis. **Biomaterials**. 26 (25): 5251-5258.

Kadyrov, M.A., N. Muratova Kh and D. Shakirov. 1966. On Obtaining a Model Osteomyelitis. **Eksp Khir Anesteziol**. 11 (6): 32-33.

Kaim, A., H.P. Ledermann, G. Bongartz, P. Messmer, J. Muller-Brand and W. Steinbrich. 2000. Chronic Post-Traumatic Osteomyelitis of the Lower Extremity: Comparison of Magnetic Resonance Imaging and Combined Bone Scintigraphy/Immunoscintigraphy with Radiolabelled Monoclonal Antigranulocyte Antibodies. **Skeletal Radiol**. 29 (7): 378-386.

Kaiser, S. and M. Rosenborg. 1994. Early Detection of Subperiosteal Abscesses by Ultrasonography. A Means for Further Successful Treatment in Pediatric Osteomyelitis. **Pediatr Radiol**. 24 (5): 336-339.

Kaito, T., A. Myoui, K. Takaoka, N. Saito, M. Nishikawa, N. Tamai, H. Ohgushi and H. Yoshikawa. 2005. Potentiation of the Activity of Bone Morphogenetic Protein-2 in Bone Regeneration by a Pla-Peg/Hydroxyapatite Composite. **Biomaterials**. 26 (1): 73-79.

Kanellakopoulou, K., I. Galanopoulos, V. Soranoglou, T. Tsaganos, V. Tziortzioti, I. Maris, A. Papalois, H. Giamarellou and E.J. Giamarellos-Bourboulis. 2009. Treatment of Experimental Osteomyelitis Caused by Methicillin-Resistant Staphylococcus Aureus with a Synthetic Carrier of Calcium Sulphate (Stimulan) Releasing Moxifloxacin. **Int J Antimicrob Agents**. 33 (4): 354-359.

Karageorgiou, V. and D. Kaplan. 2005. Porosity of 3d Biomaterial Scaffolds and Osteogenesis. **Biomaterials**. 26 (27): 5474-5491.

Kaya, M., G. Simsek-Kaya, N. Gursan, E. Kirecci, E. Dayi and B. Gundogdu. 2011. Local Treatment of Chronic Osteomyelitis with Surgical Debridement and Tigecycline-Impregnated Calcium Hydroxyapatite: An Experimental Study. **Oral Surg Oral Med Oral Pathol Oral Radiol Endod**. 113 (2): 340-347

Kelly, P.J. 1984. Infected Nonunion of the Femur and Tibia. **Orthop Clin North Am**. 15 (3): 481-490.

Kelsey, R., A. Kor and F. Cordano. 1995. Hematogenous Osteomyelitis of the Calcaneus in Children: Surgical Treatment and Use of Implanted Antibiotic Beads. **J Foot Ankle Surg**. 34 (6): 547-555.

Klemm, K.W. 1993. Antibiotic Bead Chains. **Clin Orthop Relat Res**. 295: 63-76.

Koo, K.H., J.W. Yang, S.H. Cho, H.R. Song, H.B. Park, Y.C. Ha, J.D. Chang, S.Y. Kim and Y.H. Kim. 2001. Impregnation of Vancomycin, Gentamicin, and Cefotaxime in a Cement Spacer for Two-Stage Cementless Reconstruction in Infected Total Hip Arthroplasty. **J Arthroplasty**. 16 (7): 882-892.

Kusmanto, F., G. Walker, Q. Gan, P. Walsh, F. Buchanan, G. Dickson, M. McCaique, C. Maggs and M. Dring. 2008. Development of Composite Tissue Scaffolds

Containing Naturally Sourced Microporous Hydroxyapatite. **Chamical engineering journal**. 139: 398-407

Lazary, A., B. Balla, J.P. Kosa, K. Bacsi, Z. Nagy, I. Takacs, P.P. Varga, G. Speer and P. Lakatos. 2007. Effect of Gypsum on Proliferation and Differentiation of MC3T3-E1 Mouse Osteoblastic Cells. **Biomaterials**. 28 (3): 393-399.

Lazzarini, L., J.T. Mader and J.H. Calhoun. 2004. Osteomyelitis in Long Bones. **J Bone Joint Surg Am**. 86-A (10): 2305-2318.

Lazzarini, L., B.A. Lipsky and J.T. Mader. 2005. Antibiotic Treatment of Osteomyelitis: What Have We Learned from 30 Years of Clinical Trials? **Int J Infect Dis**. 9 (3): 127-138.

Le Nihouannen, D., G. Daculsi, A. Saffarzadeh, O. Gauthier, S. Delplace, P. Pilet and P. Layrolle. 2005. Ectopic Bone Formation by Microporous Calcium Phosphate Ceramic Particles in Sheep Muscles. **Bone**. 36 (6): 1086-1093.

Lee, G.H., J.G. Khoury, J.E. Bell and J.A. Buckwalter. 2002. Adverse Reactions to Osteoset Bone Graft Substitute, the Incidence in a Consecutive Series. **Iowa Orthop J**. 22: 35-38.

Lee, S.Y., J.Y. Koak, S.J. Heo, S.K. Kim, S.J. Lee and S.Y. Nam. 2010. Osseointegration of Anodized Titanium Implants Coated with Poly(Lactide-Co-Glycolide)/Basic Fibroblast Growth Factor by Electrospray. **Int J Oral Maxillofac Implants**. 25 (2): 315-320.

Lew, D.P. and F.A. Waldvogel. 2004. Osteomyelitis. **Lancet**. 364 (9431): 369-379.

Lucke, M., G. Schmidmaier, S. Sadoni, B. Wildemann, R. Schiller, N.P. Haas and M. Raschke. 2003. Gentamicin Coating of Metallic Implants Reduces Implant-Related Osteomyelitis in Rats. **Bone**. 32 (5): 521-531.

MacNeill, S.R., C.M. Cobb, J.W. Rapley, A.G. Glaros and P. Spencer. 1999. In Vivo Comparison of Synthetic Osseous Graft Materials. A Preliminary Study. **J Clin Periodontol**. 26 (4): 239-245.

Mader, J.T., M.E. Shirtliff, S.C. Bergquist and J. Calhoun. 1999. Antimicrobial Treatment of Chronic Osteomyelitis. **Clin Orthop Relat Res**. 360: 47-65.

Mader, J.T., C.M. Stevens, J.H. Stevens, R. Ruble, J.T. Lathrop and J.H. Calhoun. 2002. Treatment of Experimental Osteomyelitis with a Fibrin Sealant Antibiotic Implant. **Clin Orthop Relat Res**. 403: 58-72.

Mah, E.T., G.W. LeQuesne, R.J. Gent and D.C. Paterson. 1994. Ultrasonic Features of Acute Osteomyelitis in Children. **J Bone Joint Surg Br**. 76 (6): 969-974.

Mahler, D.B. and A.B. Ady. 1960. An Explanation for the Hygroscopic Setting Expansion of Dental Gypsum Products. **J Dent Res**. 39: 578-589.

Malizos, K.N., N.E. Gougoulias, Z.H. Dailiana, S. Varitimidis, K.A. Bargiotas and D. Paridis. 2010. Ankle and Foot Osteomyelitis: Treatment Protocol and Clinical Results. **Injury**. 41 (3): 285-293.

Mast, N.H. and D. Horwitz. 2002. Osteomyelitis: A Review of Current Literature and Concepts. **Operative techniques in orthopaedics**. 12 (4): 232-241.

May, J.W., J.B. Jupiter, A.J. Weiland and H.S. Byrd. 1989. Clinical Classification of Post-Traumatic Tibial Osteomyelitis. **J Bone Joint Surg Am**. 71 (9): 1422-1428.

McLaren, A.C., S.G. McLaren and M.K. Hickmon. 2007. Sucrose, Xylitol, and Erythritol Increase Pmma Permeability for Depot Antibiotics. **Clin Orthop Relat Res**. 461: 60-63.

McLaren, A.C., C.L. Nelson, S.G. McLaren and C.G.R. De. 2004. The Effect of Glycine Filler on the Elution Rate of Gentamicin from Acrylic Bone Cement: A Pilot Study. **Clin Orthop Relat Res**. 427: 25-27.

McNally, M. and K. Nagarajah. 2010. Osteomyelitis. **Orthopedics and trauma**. 24 (6): 416-429.

Mendel, V., B. Reichert, H.J. Simanowski and H.C. Scholz. 1999. Therapy with Hyperbaric Oxygen and Cefazolin for Experimental Osteomyelitis Due to Staphylococcus Aureus in Rats. **Undersea Hyperb Med**. 26 (3): 169-174.

Meyer, J.D., R.F. Falk, R.M. Kelly, J.E. Shively, S.J. Withrow, W.S. Dernell, D.J. Kroll, T.W. Randolph and M.C. Manning. 1998. Preparation and in Vitro Characterization of Gentamycin-Impregnated Biodegradable Beads Suitable for Treatment of Osteomyelitis. **J Pharm Sci**. 87 (9): 1149-1154.

Monzon, M., F. Garcia-Alvarez, A. Lacleriga, E. Gracia, J. Leiva, C. Oteiza and B. Amorena. 2001. A Simple Infection Model Using Pre-Colonized Implants to Reproduce Rat Chronic Staphylococcus Aureus Osteomyelitis and Study Antibiotic Treatment. **J Orthop Res**. 19 (5): 820-826.

Mudun, A., S. Unal, R. Aktay, S. Akmehmet and S. Cantez. 1995. Tc-99m Nanocolloid and Tc-99m Mdp Three-Phase Bone Imaging in Osteomyelitis and Septic Arthritis. A Comparative Study. **Clin Nucl Med**. 20 (9): 772-778.

Nandi, S.K., B. Kundu, S.K. Ghosh, T.K. Mandal, S. Datta, D.K. De and D. Basu. 2009. Cefuroxime-Impregnated Calcium Phosphates as an Implantable Delivery System in Experimental Osteomyelitis. **Ceramics International**. 35: 1367-1376.

Nandi, S.K., P. Mukherjee, S. Roy and B. Kundu. 2009. Local Antibiotic Delivery Systems for the Treatment of Osteomyelitis - a Review. **Materials Science and Engineering C**. 29: 2478–2485.

Nelson, C.L., S.G. McLaren, R.A. Skinner, M.S. Smeltzer, J.R. Thomas and K.M. Olsen. 2002. The Treatment of Experimental Osteomyelitis by Surgical Debridement and the Implantation of Calcium Sulfate Tobramycin Pellets. **J Orthop Res**. 20 (4): 643-647.

Nelson, D.R., T.B. Buxton, Q.N. Luu and J.P. Rissing. 1990. The Promotional Effect of Bone Wax on Experimental Staphylococcus Aureus Osteomyelitis. **J Thorac Cardiovasc Surg**. 99 (6): 977-980.

Noel, S.P., H. Courtney, J.D. Bumgardner and W.O. Haggard. 2008. Chitosan Films: A Potential Local Drug Delivery System for Antibiotics. **Clin Orthop Relat Res**. 466 (6): 1377-1382.

Norden, C.W. 1970. Experimental Osteomyelitis. I. A Description of the Model. **J Infect Dis**. 122 (5): 410-418.

Nyan, M., D. Sato, M. Oda, T. Machida, H. Kobayashi, T. Nakamura and S. Kasugai. 2007. Bone Formation with the Combination of Simvastatin and Calcium Sulfate in Critical-Sized Rat Calvarial Defect. **J Pharmacol Sci**. 104 (4): 384-386.

Orhan, Z., E. Cevher, A. Yildiz, R. Ahiskali, D. Sensoy and L. Mulazimoglu. 2009. Biodegradable Microspherical Implants Containing Teicoplanin for the Treatment

of Methicillin-Resistant Staphylococcus Aureus Osteomyelitis. **Arch Orthop Trauma Surg**. 130 (1): 135-142

Orsini, G., J. Ricci, A. Scarano, G. Pecora, G. Petrone, G. Iezzi and A. Piattelli. 2004. Bone-Defect Healing with Calcium-Sulfate Particles and Cement: An Experimental Study in Rabbit. **J Biomed Mater Res B Appl Biomater**. 68 (2): 199-208.

Osaki, S., M. Chen and P.O. Zamora. 2012. Controlled Drug Release through a Plasma Polymerized Tetramethylcyclo-Tetrasiloxane Coating Barrier. **J Biomater Sci Polym Ed**. 23 (1-4): 483-496.

Park, Y.B., K. Mohan, A. Al-Sanousi, B. Almaghrabi, R.J. Genco, M.T. Swihart and R. Dziak. 2011. Synthesis and Characterization of Nanocrystalline Calcium Sulfate for Use in Osseous Regeneration. **Biomed Mater**. 6 (5): 055007.

Pecora, G., S. Andreana, J.E. Margarone, U. Covani and J.S. Sottosanti. 1997. Bone Regeneration with a Calcium Sulfate Barrier. **Oral Surg Oral Med Oral Pathol Oral Radiol Endod**. 84 (4): 424-429.

Peltier, L.F. 1961. The Use of Plaster of Paris to Fill Defects in Bone. **Clin Orthop**. 21: 1-31.

Peters, A.M. 1998. The Use of Nuclear Medicine in Infections. **Br J Radiol**. 71 (843): 252-261.

Petruskevicius, J., S. Nielsen, S. Kaalund, P.R. Knudsen and S. Overgaard. 2002. No Effect of Osteoset, a Bone Graft Substitute, on Bone Healing in Humans: A Prospective Randomized Double-Blind Study. **Acta Orthop Scand**. 73 (5): 575-578.

Rasyid, H.N., H.C. van der Mei, H.W. Frijlink, S. Soegijoko, J.R. van Horn, H.J. Busscher and D. Neut. 2009. Concepts for Increasing Gentamicin Release from Handmade Bone Cement Beads. **Acta Orthop**. 80 (5): 508-513.

Rauschmann, M.A., T.A. Wichelhaus, V. Stirnal, E. Dingeldein, L. Zichner, R. Schnettler and V. Alt. 2005. Nanocrystalline Hydroxyapatite and Calcium Sulphate as Biodegradable Composite Carrier Material for Local Delivery of Antibiotics in Bone Infections. **Biomaterials**. 26 (15): 2677-2684.

Reignier, J. and M.A. Huneault. 2006. Preparation of Interconnected Poly(3-Caprolactone) Porous Scaffolds by a Combination of Polymer and Salt Particulate Leaching. **Polymer**. 47: 4703–4717.

Rissing, J.P., T.B. Buxton, R.S. Weinstein and R.K. Shockley. 1985. Model of Experimental Chronic Osteomyelitis in Rats. **Infect Immun**. 47 (3): 581-586.

Robiller, F.C., K.D. Stumpe, T. Kossmann, D. Weisshaupt, E. Bruder and G.K. von Schulthess. 2000. Chronic Osteomyelitis of the Femur: Value of Pet Imaging. **Eur Radiol**. 10 (5): 855-858.

Robinson, D., D. Alk, J. Sandbank, R. Farber and N. Halperin. 1999. Inflammatory Reactions Associated with a Calcium Sulfate Bone Substitute. **Ann Transplant**. 4 (3-4): 91-97.

Roeder, B., C.C. Van Gils and S. Maling. 2000. Antibiotic Beads in the Treatment of Diabetic Pedal Osteomyelitis. **J Foot Ankle Surg**. 39 (2): 124-130.

Salgami, E.V., F.L. Bowling, R.W. Whitehouse and A.J. Boulton. 2007. Use of Tobramycin-Impregnated Calcium Sulphate Pellets in Addition to Oral Antibiotics: An Alternative Treatment to Minor Amputation in a Case of Diabetic Foot Osteomyelitis. **Diabetes Care**. 30 (1): 181-182.

Santiago, R.C., C.R. Gimenez and K. McCarthy. 2003. Imaging of Osteomyelitis and Musculoskeletal Soft Tissue Infections: Current Concepts. **Rheum Dis Clin North Am**. 29 (1): 89-109.

Santschi, E.M. and L. McGarvey. 2003. In Vitro Elution of Gentamicin from Plaster of Paris Beads. **Vet Surg**. 32 (2): 128-133.

Schmitz, A., T. Kalicke, P. Willkomm, F. Grunwald, J. Kandyba and O. Schmitt. 2000. Use of Fluorine-18 Fluoro-2-Deoxy-D-Glucose Positron Emission Tomography in Assessing the Process of Tuberculous Spondylitis. **J Spinal Disord**. 13 (6): 541-544.

Schurman, D.J., C. Trindade, H.P. Hirshman, K. Moser, G. Kajiyama and P. Stevens. 1978. Antibiotic-Acrylic Bone Cement Composites. Studies of Gentamicin and Palacos. **J Bone Joint Surg Am.** 60 (7): 978-984.

Shiramizu, K., V. Lovric, A. Leung and W.R. Walsh. 2008. How Do Porosity-Inducing Techniques Affect Antibiotic Elution from Bone Cement? An in Vitro Comparison between Hydrogen Peroxide and a Mechanical Mixer. **J Orthop Traumatol**. 9 (1): 17-22.

Shvyrkov, M.B., A. Shamsudinov and D.D. Sumarokov. 1981. Phosphorus-Calcium Metabolism in Traumatic Osteomyelitis of the Mandible. **Stomatologiia (Mosk)**. 60 (2): 23-25.

Sia, I.G. and E.F. Berbari. 2006. Infection and Musculoskeletal Conditions: Osteomyelitis. **Best Pract Res Clin Rheumatol**. 20 (6): 1065-1081.

Sidqui, M., P. Collin, C. Vitte and N. Forest. 1995. Osteoblast Adherence and Resorption Activity of Isolated Osteoclasts on Calcium Sulphate Hemihydrate. **Biomaterials**. 16 (17): 1327-1332.

Smeltzer, M.S., J.R. Thomas, S.G. Hickmon, R.A. Skinner, C.L. Nelson, D. Griffith, T.R. Jr. Parr and R.P. Evans. 1997. Characterization of a Rabbit Model of Staphylococcal Osteomyelitis. **J Orthop Res**. 15 (3): 414-421.

Strocchi, R., G. Orsini, G. Iezzi, A. Scarano, C. Rubini, G. Pecora and A. Piattelli. 2002. Bone Regeneration with Calcium Sulfate: Evidence for Increased Angiogenesis in Rabbits. **J Oral Implantol**. 28 (6): 273-278.

Takahashi, Y. and Y. Tabata. 2004. Effect of the Fiber Diameter and Porosity of Non-Woven Pet Fabrics on the Osteogenic Differentiation of Mesenchymal Stem Cells. **J Biomater Sci Polym Ed**. 15 (1): 41-57.

Thitiyanaporn, C., N. Thengchaisri and P. Udomkusonsri. 2012. Effect of Porosity of Calcium Sulfate Beads on Ceftazidime Elution and in Vitro Osteogenic Properties. **Kasetsart journal (Natural science)**. 46 (5): 703-714.

Thomas, M.V. and D.A. Puleo. 2009. Calcium Sulfate: Properties and Clinical Applications. **J Biomed Mater Res B Appl Biomater**. 88 (2): 597-610.

Tuzuner, T., I. Uygur, I. Sencan, U. Haklar, B. Oktas and D. Ozdemir. 2007. Elution Characteristics and Mechanical Properties of Calcium Sulfate-Loaded Bone Cement Containing Teicoplanin. **J Orthop Sci**. 12 (2): 170-177.

Udomkusonsri, P., S. Kaewmokul, S. Arthitvong and T. Songserm. 2010. Use of Enrofloxacin in Calcium Beads for Local Infection Therapy in Animals. **Kasetsart Journal (Natural Science)**. 44: 1115-1120.

Unkila-Kallio, L., M.J. Kallio, J. Eskola and H. Peltola. 1994. Serum C-Reactive Protein, Erythrocyte Sedimentation Rate, and White Blood Cell Count in Acute Hematogenous Osteomyelitis of Children. **Pediatrics**. 93 (1): 59-62.

Urban, R.M., T.M. Turner, D.J. Hall, S.I. Infanger, N. Cheema, T.H. Lim, J. Moseley, M. Carroll and M. Roark. 2004. Effects of Altered Crystalline Structure and Increased Initial Compressive Strength of Calcium Sulfate Bone Graft Substitute Pellets on New Bone Formation. **Orthopedics**. 27 (Suppl1): S113-118.

van de Belt, H., D. Neut, D.R. Uges, W. Schenk, J.R. van Horn, H.C. van der Mei and H.J. Busscher. 2000. Surface Roughness, Porosity and Wettability of Gentamicin-Loaded Bone Cements and Their Antibiotic Release. **Biomaterials**. 21 (19): 1981-1987.

Vasilev, K., N. Poulter, P. Martinek and H.J. Griesser. 2011. Controlled Release of Levofloxacin Sandwiched between Two Plasma Polymerized Layers on a Solid Carrier. **ACS Appl Mater Interfaces**. 3 (12): 4831-4836.

Wahlig, H. and E. Dingeldein. 1980. Antibiotics and Bone Cements. Experimental and Clinical Long-Term Observations. **Acta Orthop Scand**. 51 (1): 49-56.

Waldvogel, F.A., G. Medoff and M.N. Swartz. 1970. Osteomyelitis: A Review of Clinical Features, Therapeutic Considerations and Unusual Aspects. **N Engl J Med**. 282 (4): 198-206.

Walsh, W.R., P. Morberg, Y. Yu, J.L. Yang, W. Haggard, P.C. Sheath, M. Svehla and W.J. Bruce. 2003. Response of a Calcium Sulfate Bone Graft Substitute in a Confined Cancellous Defect. **Clin Orthop Relat Res**. 406: 228-236.

Wichelhaus, T.A., E. Dingeldein, M. Rauschmann, S. Kluge, R. Dieterich, V. Schafer and V. Brade. 2001. Elution Characteristics of Vancomycin, Teicoplanin, Gentamicin and Clindamycin from Calcium Sulphate Beads. **J Antimicrob Chemother**. 48 (1): 117-119.

Xie, Z., X. Liu, W. Jia, C. Zhang, W. Huang and J. Wang. 2009. Treatment of Osteomyelitis and Repair of Bone Defect by Degradable Bioactive Borate Glass Releasing Vancomycin. **J Control Release**. 139 (2): 118-126.

CURRICULUM VITAE

NAME : Mr. Chaiyakorn Thitiyanaporn

BIRTH DATE : September 27, 1979

BIRTH PLACE : Bangkok, Thailand

EDUCATION	**: YEAR**	**INSTITUTE**	**DEGREE/DIPLOMA**
	2002	Kasetsart University	D.V.M. (First class honor)

POSITION/TITLE : Lecturer

WORK PLACE : Department of Companion Animal Clinical Sciences, Faculty of Veterinary Medicine, Kasetsart University

SCHOLARSHIP/AWARD : Strategic Scholarships Fellowships Frontier Research Network, Office of the Higher Education Commission, Ministry of Education, Thailand.

PUBLICATION :

Thitiyanaporn, C., N. Thengchaisri and P. Udomkusonsri. 2012. Effect of Porosity of Calcium Sulfate Beads on Ceftazidime Elution and in Vitro Osteogenic Properties. **Kasetsart journal (Natural science)**. 46 (5): 703-714